

Quantum–classical correspondence in spin–boson equilibrium states at arbitrary coupling

F. Cerisola,^{1,2,*} M. Berritta,¹ S. Scali,¹ S.A.R. Horsley,¹ J.D. Cresser,^{1,3,4} and J. Anders^{1,5}

¹*Department of Physics and Astronomy, University of Exeter, Stocker Road, Exeter EX4 4QL, UK*

²*Department of Materials, University of Oxford, Parks Road, Oxford OX1 3PH, United Kingdom*

³*School of Physics and Astronomy, University of Glasgow, Glasgow, G12 8QQ, UK*

⁴*Department of Physics and Astronomy, Macquarie University, 2109 NSW, Australia*

⁵*Institut für Physik und Astronomie, University of Potsdam, 14476 Potsdam, Germany*

(Dated: July 13, 2022)

It is known that the equilibrium properties of nanoscale systems can deviate significantly from standard thermodynamics due to their coupling to an environment. For the generalised θ -angled spin-boson model, here we derive an explicit form of the classical mean force equilibrium state. Taking the large spin limit of the quantum spin-boson model, we demonstrate that the quantum-classical correspondence is maintained at arbitrary coupling strength. This correspondence gives insight into the conditions for a quantum system to be well-approximated by its classical counterpart. We further demonstrate that, counterintuitively, previously identified environment-induced ‘coherences’ in the equilibrium state of weakly coupled quantum spins, do *not* disappear in the classical case. Finally, we categorise various coupling regimes, from ultra-weak to ultra-strong, and find that the same value of coupling strength can either be ‘weak’ or ‘strong’, depending on whether the system is quantum or classical. Our results shed light on the interplay of quantum and mean force corrections in equilibrium states of the spin-boson model, and will help draw the quantum to classical boundary in a range of fields, such as magnetism and exciton dynamics.

Bohr’s correspondence principle [1] played an essential role in the early development of quantum mechanics. Since then, a variety of interpretations and applications of the correspondence principle have been explored [2–9]. One form asks if the statistical properties of a quantum system approach those of its classical counterpart in the limit of large quantum numbers [4, 5]. This question was answered affirmatively by Millard and Leff, and Lieb for a quantum spin system [2, 3]. They proved that the system’s thermodynamic partition function Z_S^{qu} associated with the Gibbs state, converges to the corresponding classical partition function Z_S^{cl} , in the limit of large spins. Such correspondence gives insight into the conditions for a quantum thermodynamic system to be well-approximated by its classical counterpart [8, 9]. While Z_S^{qu} is computationally tough to evaluate for many systems, Z_S^{cl} offers tractable expressions with which thermodynamic properties, such as free energies, susceptibilities and correlation functions, can readily be computed [2, 3]. Similarly, many dynamical approaches solve a classical problem rather than the much harder quantum problem. For example, sophisticated atomistic simulations of the magnetisation dynamics in magnetic materials [10–14] solve the evolution of millions of interacting classical spins. A corresponding quantum simulation [15] would require no less than a full-blown quantum computer as its hardware.

Meanwhile, in the field of quantum thermodynamics, extensive progress has recently been made in constructing a comprehensive framework of “strong coupling thermodynamics” for classical [16–21] and quantum [22–32] systems. This framework extends standard thermodynamic relations to systems whose coupling to a thermal environment can not be neglected. The equilibrium state is then no longer the quantum or classical

Gibbs state, but must be replaced with the environment-corrected mean force (Gibbs) state [31–33]. These modifications bring into question the validity of the correspondence principle when the environment-coupling is no longer negligible. Mathematically, the challenge is that in addition to tracing over the system, one must also evaluate the trace over the environment.

Strong coupling contributions are present for both classical and quantum systems. However, a quantitative characterisation of the difference between these two predictions, in various coupling regimes, is missing. For example, apart from temperature, what are the parameters controlling the deviations between the quantum and classical spin expectation values? Do coherences, found to persist in the mean force equilibrium state of a quantum system [34], decohere when taking the classical limit? And are the coupling regimes, from weak to ultrastrong coupling [33], the same for the classical and quantum case? In this paper, we answer these questions for the particular case of a spin S_0 coupled to a one-dimensional bosonic environment such that both dephasing and detuning can occur (θ -angled spin-boson model).

Setting. This generalised version of the spin-boson model [35, 36] describes a vast range of physical contexts, including excitation energy transfer processes in molecular aggregates described by the Frenkel exciton Hamiltonian [37–43], the electronic occupation of a double quantum dot whose electronic dipole moment couples to the substrate phonons in a semiconductor [34], an electronic, nuclear or effective spin exposed to a magnetic field and interacting with an (anisotropic) phononic, electronic or magnonic environment [44], and a plethora of other aspects of quantum dots, ultracold atomic impurities, and superconducting circuits [45–48]. In all these contexts, an effective “spin” S interacts with an environment, where S is a vector of operators (with units of angular mo-

* federico.cerisola@eng.ox.ac.uk

mentum) whose components fulfil the angular momentum commutation relations $[S_j, S_k] = i\hbar \sum_l \epsilon_{jkl} S_l$ with $j, k, l = x, y, z$. We will consider spins of any length S_0 , i.e. $\mathbf{S}^2 = S_0(S_0 + \hbar)\mathbf{1}$. The system Hamiltonian is

$$H_S = -\omega_L S_z, \quad (1)$$

where the system energy level spacing is $\hbar\omega_L > 0$ and the energy axis is in the $-z$ -direction without loss of generality. For a double quantum dot, the frequency ω_L is determined by the energetic detuning and the tunneling between the dots [34]. For an electron spin with $S_0 = \hbar/2$, the energy gap is set by a (negative) gyromagnetic ratio γ and an external magnetic field $\mathbf{B}_{\text{ext}} = -B_{\text{ext}}\hat{\mathbf{z}}$, such that $\omega_L = \gamma B_{\text{ext}}$ is the Larmor frequency.

The spin system is in contact with a bosonic reservoir, which is responsible for the dissipation and equilibration of the system. Typically, this environment will consist of phononic modes or an electromagnetic field [32, 49]. The bare Hamiltonian of the reservoir degrees of freedom is

$$H_R = \frac{1}{2} \int_0^\infty d\omega (P_\omega^2 + \omega^2 X_\omega^2), \quad (2)$$

where X_ω and P_ω are the position and momentum operators of the reservoir mode at frequency ω which satisfy the canonical commutation relations $[X_\omega, P_{\omega'}] = i\hbar \delta(\omega - \omega')$. With the identifications made in (1) and (2), the system-reservoir Hamiltonian is

$$H_{\text{tot}} = H_S + H_R + H_{\text{int}}, \quad (3)$$

which contains a system-reservoir coupling H_{int} . Physically, the coupling can often be approximated to be linear in the canonical reservoir operators [32], and is then modelled as [34, 49, 50]

$$H_{\text{int}} = S_\theta \int_0^\infty d\omega C_\omega X_\omega, \quad (4)$$

where the coupling function C_ω determines the interaction strength between the system and each reservoir mode ω . C_ω is related to the reservoir spectral density J_ω via $J_\omega = C_\omega^2/(2\omega)$.

It is important to note that the coupling is to the spin (component) operator $S_\theta = S_z \cos \theta - S_x \sin \theta$ which is at an angle θ with respect to system's bare energy axis, see Fig. 1. For example, for a double quantum dot [34], the angle θ is determined by the ratio of detuning and tunnelling parameters.

In what follows we will need an integrated form of the spectral density, namely

$$Q = \int_0^\infty d\omega \frac{J_\omega}{\omega} = \int_0^\infty d\omega \frac{C_\omega^2}{2\omega^2}. \quad (5)$$

This quantity is a measure of the strength of the system-environment coupling and it is sometimes called “reorganization energy” [33, 51–53]. The analytical results discussed below are valid for arbitrary coupling functions C_ω (or reorganisation energies Q), while the figures assume couplings of Lorentzian form [44], see Supplement D.

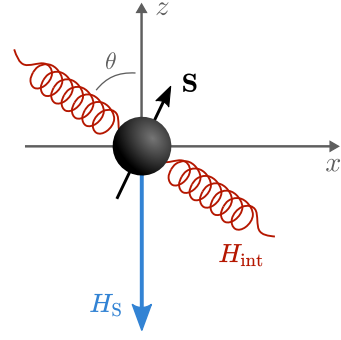


FIG. 1. **Illustration of bare and interaction energy axes.** A spin operator (vector) \mathbf{S} with system Hamiltonian H_S with energy axis in z -direction is coupled in θ -direction to a bosonic environment via H_{int} .

We will model H_{tot} (Eq. (3)) either fully quantum mechanically as detailed above, or fully classically. To obtain the classical case, the spin \mathbf{S} operator will be replaced by a three-dimensional vector of length S_0 , and the reservoir operators X_ω and P_ω will be replaced by classical phase-space coordinates. Below, we evaluate the spin's so-called mean force (Gibbs) states, CMF and QMF, for the classical and quantum case, respectively. The mean force approach postulates [32] that the equilibrium state of a system in contact with a reservoir at temperature T is the mean force (MF) state, defined as

$$\tau_{\text{MF}} := \text{tr}_R[\tau_{\text{tot}}] = \text{tr}_R \left[\frac{e^{-\beta H_{\text{tot}}}}{Z_{\text{tot}}} \right]. \quad (6)$$

That is, τ_{MF} is the reduced system state of the global Gibbs state τ_{tot} , where $\beta = 1/k_B T$ is the inverse temperature with k_B the Boltzmann constant, and Z_{tot} is the global partition function. Quantum mechanically, tr_R stands for the operator trace over the reservoir space while classically, “tracing” is done by integrating over the reservoir degrees of freedom. Further detail on classical and quantum tracing for the spin and the reservoir, respectively, is given in Supplement A.

While the formal definition of τ_{MF} is deceptively simple, carrying out the trace over the reservoir – to obtain a quantum expression of τ_{MF} in terms of system operators alone – is notoriously difficult. Often, expansions for weak coupling are made [22, 34]. For a general quantum system (i.e. not necessarily a spin), an expression of τ_{MF} has recently been derived in this limit [33]. Furthermore, recent progress has been made on expressions of the quantum τ_{MF} in the limit of ultrastrong coupling [33], and for large but finite coupling [31, 32, 54]. Moreover, high temperature expansions have been derived that are also valid at intermediate coupling strengths [43]. However, the low and intermediate temperature form of the quantum τ_{MF} for intermediate coupling is not known, neither in general nor for the θ -angled spin boson model.

Classical MF state at arbitrary coupling. In contrast, here we show that the analogous problem of a *classical* spin vector of arbitrary length S_0 , coupled to a bosonic reservoir via Eq. (4), is tractable for arbitrary

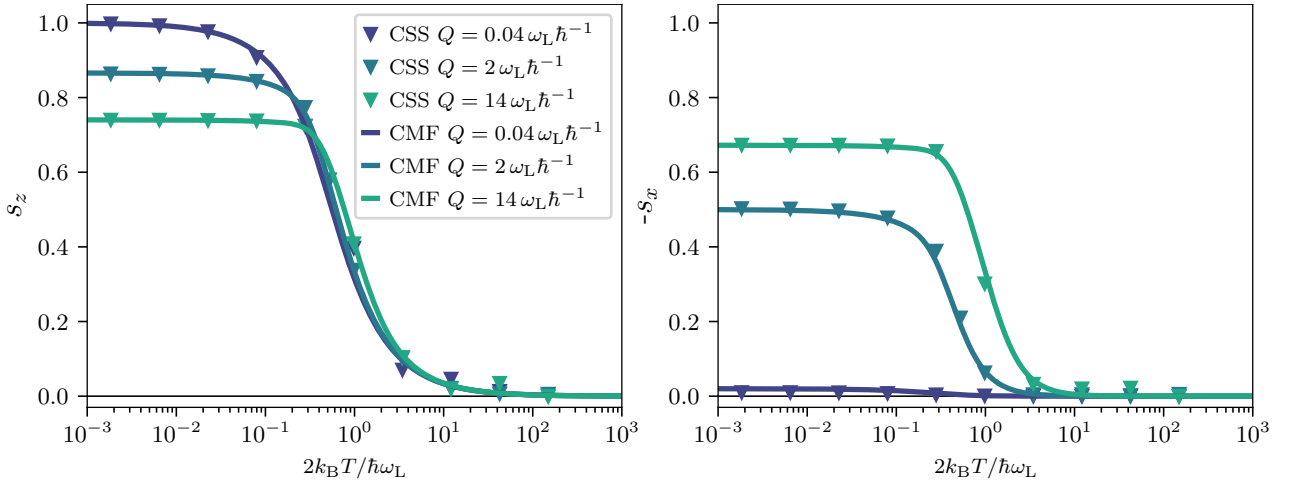


FIG. 2. **Mean force and steady-state spin expectation values for different coupling strengths.** Normalised expectation values of the classical spin components z (left) and x (right) as a function of temperature. These are obtained with: (CSS) the long time average of the dynamical evolution of the spin, $s_k = \langle S_k \rangle_{\text{CSS}}/S_0$; and (CMF) the classical MF state (Eq. (7)), $s_k = \langle S_k \rangle_{\text{MF}}/S_0$. These are shown for three different coupling strengths $Q = 0.04 \omega_L \hbar^{-1}, 2 \omega_L \hbar^{-1}, 14 \omega_L \hbar^{-1}$, that range from the weak to the strong coupling regimes. In all three cases, we see that the MF predictions are fully consistent with the results of the dynamics. All the plots are for Lorentzian coupling with $\omega_0 = 7\omega_L$, $\Gamma = 5\omega_L$, and coupling angle $\theta = 45^\circ$ (see Supplement D for details). The temperature scale shown corresponds to a spin $S_0 = \hbar/2$, but, as discussed, the CMF is invariant to a change in S_0 with the rescaling introduced in (8), and the same has been shown to hold for the dynamical equations of motion in [44], making the results here plotted effectively independent of S_0 .

coupling function C_ω and arbitrary temperature. By carrying out the (classical) partial trace over the reservoir, i.e. $\text{tr}_R^{\text{cl}}[\tau_{\text{tot}}]$, we uncover a rather compact expression for the spin's CMF state τ_{MF} and the CMF partition function \tilde{Z}_S^{cl} :

$$\tau_{\text{MF}} = \frac{e^{-\beta(H_S - Q S_\theta^2)}}{\tilde{Z}_S^{\text{cl}}} \quad (7)$$

with $\tilde{Z}_S^{\text{cl}} = \text{tr}_S^{\text{cl}}[e^{-\beta(H_S - Q S_\theta^2)}]$.

These compact classical mean force expressions, valid for arbitrarily large coupling, are the first result of this paper.

The state τ_{MF} clearly differs from the standard Gibbs state by the presence of the reorganisation energy term $-Q S_\theta^2$. The quadratic dependence on S_θ changes the character of the distribution, from a standard exponential to an exponential with a positive quadratic term, altering significantly the state whenever the system-reservoir coupling is non-negligible. [As discussed further below, Fig. 4c) visualises an example of the τ_{MF} distribution over the spin's spherical angles θ and ϕ , while the standard Gibbs distribution is shown in 4b).]

Throughout this article, we will consider that the MF state is the equilibrium state reached by a system in contact with a thermal bath. While this is widely thought to be the case, some open questions remain about formal proofs showing the convergence of the dynamics towards the steady state predicted by the MF state [32]. For example, for quantum systems, this convergence has only been proven in the weak [22] and ultrastrong limits [31], while for intermediate coupling strengths there is numerical evidence for the validity of the MF state [36]. Here, we numerically verify the convergence of the dy-

namics towards the MF state for the case of the classical spin at arbitrary coupling strength. This is possible thanks to the numerical method proposed in [44]. Fig. 2 shows the long time average of the spin components once the dynamics has reached steady state (CSS, triangles), together with the expectation values predicted by the static MF state (CMF, solid lines), for a wide range of coupling strengths going from weak to strong coupling [55]. We find that both predictions are in excellent agreement, providing strong evidence for the convergence of the dynamics towards the MF.

It remains an open problem to derive, for arbitrary coupling and temperature, analogous expressions to (7) for the *quantum* mean force state and partition function, $\tilde{Z}_S^{\text{qu}} := Z_{\text{tot}}^{\text{qu}}/Z_R^{\text{qu}}$.

Quantum-classical correspondence. We now demonstrate that the quantum partition function \tilde{Z}_S^{qu} , which includes arbitrarily large mean force corrections, converges to the classical one \tilde{Z}_S^{cl} , Eq. (7). A well-known classical limit of a quantum spin is to increase the quantum spin's length, $S_0 \rightarrow \infty$. This is because, when S_0 increases, the quantized angular momentum level spacing relative to S_0 decreases, approaching a continuum of states that can be described in terms of a classical vector [1]. What is less well known is that, at the same time, other parameters also have to be rescaled in order to obtain a non-trivial limit [56]. Such rescaling can either be applied to the Hamiltonian parameters [57], or to the inverse temperature β . We here proceed with the second approach and take $\beta' = \beta S_0$ to be a constant during the limiting process.

For the system's standard Gibbs state partition function, this rescaling leaves the classical partition function $Z_S^{\text{cl}}(\beta S_0) = \sinh(\beta S_0 \omega_L)/\beta S_0 \omega_L$ invariant, be-

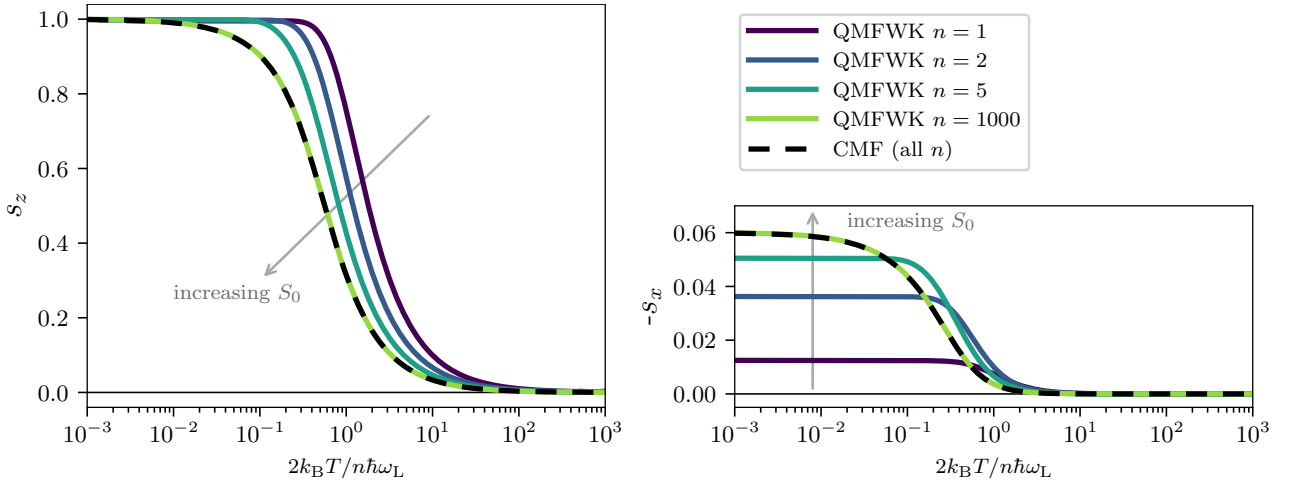


FIG. 3. **Classical and quantum mean force spin components.** Normalised expectation values of the spin components s_z (left) and s_x (right) obtained with: (QMFWK) the quantum MF partition function \tilde{Z}_S^{qu} in the weak coupling limit for a spin of length $S_0 = n\hbar/2$ ($n = 1, 2, 5, 100$); (CMF) the classical MF partition function \tilde{Z}_S^{cl} given in (7). As the length S_0 of the quantum spin is increased, the quantum mean force prediction QMFWK converges to that corresponding to the CMF state. Non-zero s_x (right) indicate “coherences” with respect to the system’s bare energy axis (z). These arise entirely due to the spin-reservoir interaction. Such coherences have been discussed for the quantum case [34]. Here we find that they also arise in the classical CMF and, comparing like with like for the same spin length $S_0 = \hbar/2$, the classical “coherences” are larger than those of the quantum spin. All plots are for a weak coupling strength, $\alpha = 0.06$, and $\theta = \pi/4$.

cause β and S_0 always appear together. In contrast, the quantum Gibbs state partition function $Z_S^{\text{qu}}(\beta, S_0) = \sinh(\beta(S_0 + \hbar/2)\omega_L) / \sinh(\beta\hbar\omega_L/2)$ is altered by the combined scaling of spin length and inverse temperature, since Z_S^{qu} separately depends on β and S_0 . In the limit $S_0 \rightarrow \infty$, one finds the convergence $\frac{\hbar}{2S_0 + \hbar} Z_S^{\text{qu}}(\beta, S_0) \rightarrow Z_S^{\text{cl}}(\beta S_0)$, as it was first proven by Millard and Leff [2] and Lieb [3] [58].

We now take a step further and consider what happens to the large S_0 limit when a non-negligible environment coupling is present. Looking at the classical MF state (7), we see that while the system energy H_S scales as S_0 , the correction that comes from the reservoir interaction H_{int} scales as QS_0^2 . Therefore, if we increased S_0 while leaving Q fixed, this would, for larger S_0 , result in a stronger reservoir interaction relative to the system energy given by H_S . Instead, we want to keep the relative energy scales of the H_S term and the coupling term QS_0^2 the same throughout the S_0 limit. For this to be true, Q must scale as

$$Q = \alpha \frac{\omega_L}{S_0}, \quad (8)$$

where α is a unit-free number that is independent of S_0 and independent of β . This scaling was also proposed in [44] to model a decreasing ratio of the “surface” of a system ($H_{\text{int}} \propto S_0 C_\omega \propto S_0 \sqrt{Q} \propto \sqrt{S_0}$) to “volume” ($H_S \propto S_0$) with increasing system size S_0 . The combined scaling of Q with S_0 , and the rescaling of the inverse temperature, $\beta S_0 = \beta' = \text{const}$, has the key property of leaving the CMF state (7) invariant.

With these ingredients, we prove the quantum-classical convergence for the MF partition functions, see Supplement E. The proof starts with the full quantum spin-reservoir partition function $Z_{\text{tot}}^{\text{qu}}$ for the total Hamil-

tonian Eq. (3). First, one finds that the combined spin-temperature rescaling leads to a well-defined classical limit of decaying commutation relations for both, system and reservoir, operators. Second, we apply a quantum-classical identity for the spin, which was originally derived for the bare spin problem by Millard & Leff with an improved proof by Lieb [2, 3]. For the coupled spin we here find that, upon shifting the reservoir modes, the trace over the reservoir separates out straightforwardly. Finally, identifying the remaining term as the classical mean force partition function given in (7), we obtain

$$\frac{\hbar}{2S_0 + \hbar} \tilde{Z}_S^{\text{qu}}(\beta, S_0) \rightarrow \tilde{Z}_S^{\text{cl}}(\beta S_0), \quad (9)$$

in the limit of $S_0 \rightarrow \infty$ while βS_0 is fixed. This quantum-classical correspondence of the mean force partition function, valid for arbitrary coupling strength α , is the second result of the paper. Details of the derivation are presented in Supplement E.

To visually illustrate the quantum to classical convergence, we choose a weak coupling strength, $\alpha = 0.06$, for which an analytical form of the quantum \tilde{Z}_S^{qu} is known [33], see Supplement I. Mean force spin component expectation values $s_k \equiv \langle S_k \rangle_{\text{MF}} / S_0$ for $k = x, z$ can then readily be computed, from the partition functions \tilde{Z}_S^{qu} and \tilde{Z}_S^{cl} , respectively (see Supplement B). Fig. 3 shows s_z and s_x for various spin lengths, $S_0 = n\hbar/2$ with $n = 1, 2, 5, 1000$ for the quantum case (QMFWK, purple to green) and the classical case (CMF, dashed black). Note, that the x -axis is a correspondingly rescaled temperature, $2k_B T / (n\hbar\omega_L)$, a scaling under which the CMF remains invariant. The numerical results illustrate that the quantum s_z and s_x change with spin length $S_0 = n\hbar/2$, and indeed converge to the classical prediction in the large spin limit, $n \rightarrow \infty$.

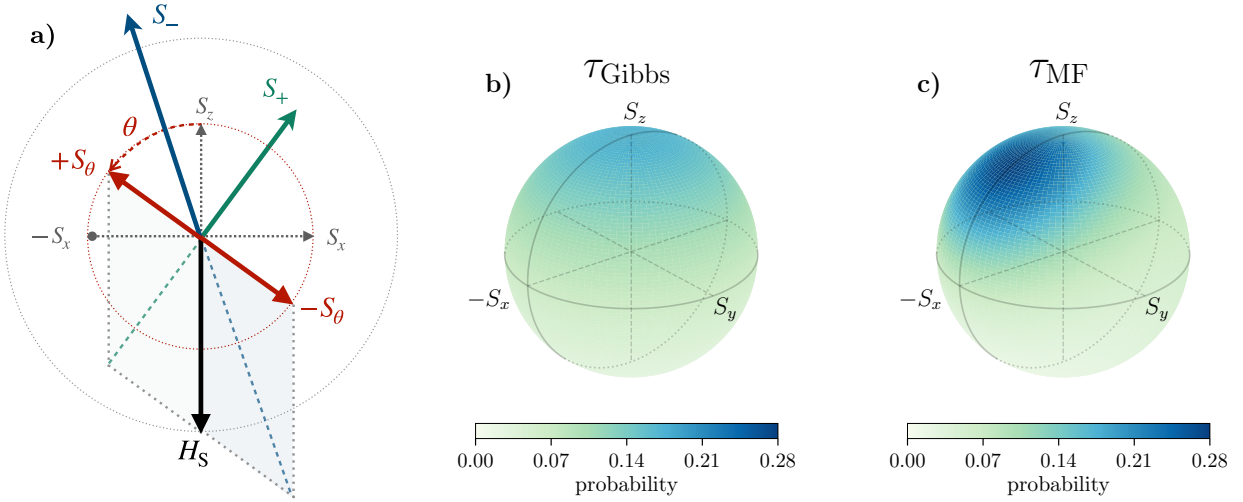


FIG. 4. **Anisotropic noise, coherences, and inhomogeneities.** **a)** A classical spin with bare system energy $H_S = -\omega_L S_z$ and interaction energy $H_{\text{int}} = S_\theta b_{\text{th}}$, with b_{th} stochastic noise induced by the environment. For $|b_{\text{th}}| < \omega_L$ (low temperature), the vector combination of noise pointing in the $+S_\theta$ -direction and the bare energy pointing in $-S_z$ -direction leads to the ground state population aligned with the S_+ -direction. Likewise, for noise in the $-S_\theta$ -direction the resulting ground state direction points in the S_- -direction, and does so with a larger magnitude. Therefore, averaging the respective thermal state populations introduces a bias that tends to align the system more with the $-S_x$ direction. Figures **a)** and **b)** show spin vector probability distributions (blue = high probability, white = low probability) as a function of three spin components on a sphere of radius S_0 . **b)** The classical Gibbs state probability distribution τ_{Gibbs} is a homogeneous function of H_S , i.e. it is constant over the energy shells of H_S which are fixed by the value of S_z . **c)** The classical mean force probability distribution τ_{MF} given in (7), peaks in a direction with positive components in $-S_x$ and S_z directions, as expected from the vector addition diagram in **a)**. This makes τ_{MF} an inhomogeneous probability distribution over the energy shells of H_S . Parameters for **b)** and **c)**: $\theta = \pi/4$, $k_B T = S_0 \omega_L$, and $Q = \omega_L / S_0$ (i.e. $\alpha = 1$).

While the existence of a quantum-classical correspondence was perhaps expected, the insight gained for the mean force states is that such transition only occurs when the reorganisation energy Q scales as $1/S_0$, cf. (8). For other scaling relations, set by the physical principles for a specific context, \tilde{Z}_S^{qu} will not converge to the classical counterpart \tilde{Z}_S^{cl} , in the large spin-temperature limit. In such case, mapping a quantum into a classical problem would require a particular renormalisation of the Hamiltonian parameters. We also note that here, we have assumed that α is independent of β . Physically this is not entirely accurate because the coupling C_ω is usually a function of temperature [59], albeit often a rather weak one. For the same limiting process to apply, a weak dependence on β would need to be compensated by an equally weak additional dependence of Q on S_0 .

Coherences and anisotropic noise. As seen in Fig. 3 (right panel), the s_x spin-component in the equilibrium state is non-zero at low temperatures, despite the fact that the bare system energy scale is set along the z -direction, see (1). Such non-zero s_x implies the presence of energetic “coherences” in the quantum system’s equilibrium state. These were recently discussed in [34, 60] for a quantum spin-1/2, i.e. $S_0 = \hbar/2$ (solid purple line in Fig. 3). Considering the quantum-classical correspondence discussed above, a natural question is whether in the classical limit one can observe “decoherence”, in the sense of vanishing coherences. However, comparing like with like, we see in Fig. 3 (right panel)

that “coherences” are also present for a classical spin with length $S_0 = \hbar/2$ (dashed black). Indeed, maybe surprisingly, classical “coherences” can be even larger in magnitude than those of a quantum spin with corresponding length S_0 .

This observation reveals that the mechanism that gives rise to these coherences is not an intrinsically quantum one. Instead, their physical origin comes from the interaction with the reservoir, even in the weak coupling limit. Specifically, we find that such coherences arise whenever the thermal noise is *anisotropic* with respect to the energy axis (S_z -axis), set by the bare system Hamiltonian (H_S). Such anisotropy occurs for any value $\theta \neq 0, \pi/2$, and independently of whether the system is quantum or classical.

To heuristically understand the origin of these coherences, we can consider the effect of the noise induced by the bath, averaging over the *populations* of effective Gibbs states associated with each instantaneous value of the noise. A figure detailing the geometry of this situation, see Fig. 4a), helps to further shed light on how classical coherences arise. The classical noise field $S_\theta b_{\text{th}}$, see Eq. (4), will take values stochastically sampled from a certain power spectrum [44]. For a given value of the noise, say $b_{\text{th}} > 0$, the spin will try to align with the effective energy axis (S_+ in Fig. 4), a combination of system energy axis and the noise axis. Sampling over time, the same noise strength $|b_{\text{th}}|$ will be applied also with a negative sign, i.e. in the $-S_\theta$ -direction, leading to a ground state orientation in the S_- -direction. Importantly, not only the direction of alignment is dif-

ferent, but additionally the strength of the effective field also differs, leading to a different ground state population. If one now takes an average over the instantaneous thermal populations for the different noise directions, these differences in populations introduce a bias. This results in the spin aligning more with the $-S_x$ -direction than with the $+S_x$ -direction, leading to a non-zero average s_x -component, a “coherence”.

We can now link the “coherences” in the classical spin system’s equilibrium state, generated by the anisotropic noise as discussed, to the concept of (in)homogeneity in an energy shell. In the context of work extraction from quantum coherences [61, 62], inhomogeneities have been identified by A. Smith, K. Sinha, C. Jarzynski as the classical analogue to quantum coherences [63]. A classical *homogeneous* probability distribution is one that has a constant value within any energy shell. In contrast, an *inhomogeneous* probability distribution is uneven within some energy shells. Fig. 4b) and 4c) show the probability density of the classical Gibbs state, $\tau_{\text{Gibbs}} \propto e^{-\beta H_S}$, and the CMF state, τ_{MF} , respectively. The energy shells for H_S are fully characterised by fixed values of S_z . Since the Gibbs state only depends on H_S , and not on S_x and S_y , it is a homogeneous distribution over the energy shells of H_S , as illustrated in Fig. 4b). On the other hand, τ_{MF} given in Eq. (7) and shown in Fig. 4c) clearly varies with S_x , illustrating the inhomogeneous nature of the CMF distribution over the energy shells of H_S .

Quantum–classical correspondence at ultrastrong coupling. We now return to the question of what parameters control the difference between the quantum and classical partition functions. Apart from temperature and spin length S_0 , we observed that the coupling to the environment introduces a new interaction energy scale, Q , into the MF partition function \tilde{Z}_S^{qu} and \tilde{Z}_S^{cl} . Numerical evaluation of s_x and s_z indicates that the difference between quantum and classical mean force spin states decreases with increasing coupling strength, see supplement Fig. S1. Indeed, as we show in Supplement J, the quantum and classical MF partition functions converge to each other (apart from irrelevant factors) in the ultrastrong limit, $Q \rightarrow \infty$. The proof proceeds via expanding the quantum MF state to lowest order in $1/Q$ [33], leading to $\tilde{Z}_{S,\text{US}}^{\text{qu}} \propto \cosh(\beta S_0 \omega_L \cos \theta)$. Notably, $\tilde{Z}_{S,\text{US}}^{\text{qu}}$ depends exclusively on the product βS_0 , implying that there is now only one energy scale, similar to what we found for the classical Gibbs \tilde{Z}_S^{cl} . An analogous expansion to obtain the ultrastrong limit for the classical case leads to $\tilde{Z}_{S,\text{US}}^{\text{cl}} \propto \tilde{Z}_{S,\text{US}}^{\text{qu}}$. Thus, in the ultrastrong limit, the mean force equilibrium properties of quantum and classical spins are the same for any fixed S_0 , without any rescaling.

Quantum limit of a classical spin. As mentioned in the introduction, simulations of quantum systems often rely on modelling the corresponding classical system in the hope the predictions may approach the quantum case. However, for small S_0 , the difference in Gibbs state predictions based on Z_S^{qu} and Z_S^{cl} is undeniable, see QG and CG in Fig. 5. On the other hand, above we observed that the interaction of a classical system

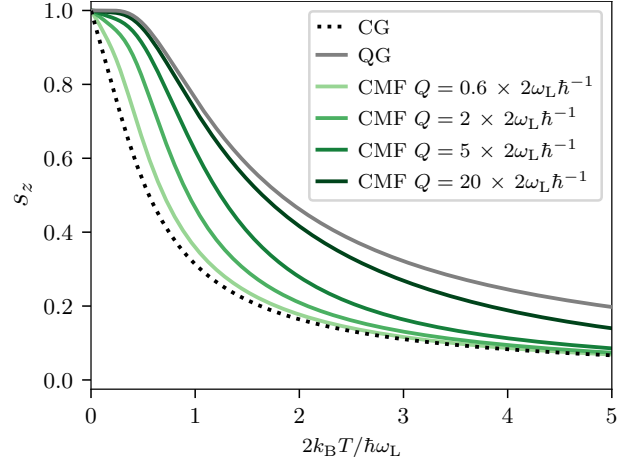


FIG. 5. **Convergence of the CMF state to the quantum Gibbs state.** The s_z -component of a spin of length $S_0 = \hbar/2$ as a function of temperature depends very significantly on whether the spin is modelled to be classical (classical Gibbs state CG, black dotted) or quantum (quantum Gibbs state, QG, grey solid). But coupling the classical spin to its environment at an angle $\theta = 0$, at increasing reorganisation energies Q , also leads to deviations (classical mean force state, CMF, solid green, darker for larger coupling Q). In the limit of infinitely large coupling (ultra-strong coupling) the CMF is found to converge to the QG state of a spin $S_0 = \hbar/2$.

with an environment changes the partition function, $Z_S^{\text{cl}} \rightarrow \tilde{Z}_S^{\text{cl}}$, just like introducing the quantum character changes the partition function, $Z_S^{\text{cl}} \rightarrow Z_S^{\text{qu}}$. One may now wonder if classical mean force predictions can approximate the quantum Gibbs state physics. Here, we show that, at least for specific settings, this is indeed possible.

We consider a classical spin of length $S_0 = \hbar/2$ and set the spin’s coupling to the reservoir to be parallel to the system energy axis (i.e. $\theta = 0$) [64]. Fig. 5 shows the s_z expectation value of the CMF state at various values of the reorganisation energy Q . As Q increases, the CMF state converges towards its ultrastrong limit with partition function $\tilde{Z}_{S,\text{US}}^{\text{cl}}(\theta = 0) \propto \cosh(\beta \hbar \omega_L / 2)$, the same as Z_S^{qu} for an uncoupled quantum spin $\hbar/2$ (see Supplement J for the detailed derivation). Interestingly, we see that, at least in this particular case, strong coupling effects of the reservoir on the classical system produce an effective behaviour that is analogous to that of a quantum spin. The possibility of extending this equilibrium state result to the dynamical state of the system remains an open question for further study.

Coupling regimes. Finally, we characterise the interaction strength that is necessary for the usual quantum Gibbs state assumption to become incorrect, and mean force corrections must be taken into account. To quantify the relative strength of coupling we use the parameter

$$\zeta = \frac{Q S_0}{\omega_L}, \quad (10)$$

which is the dimensionless ratio of interaction and bare energy terms, see also Eq. (7). For the specific case of

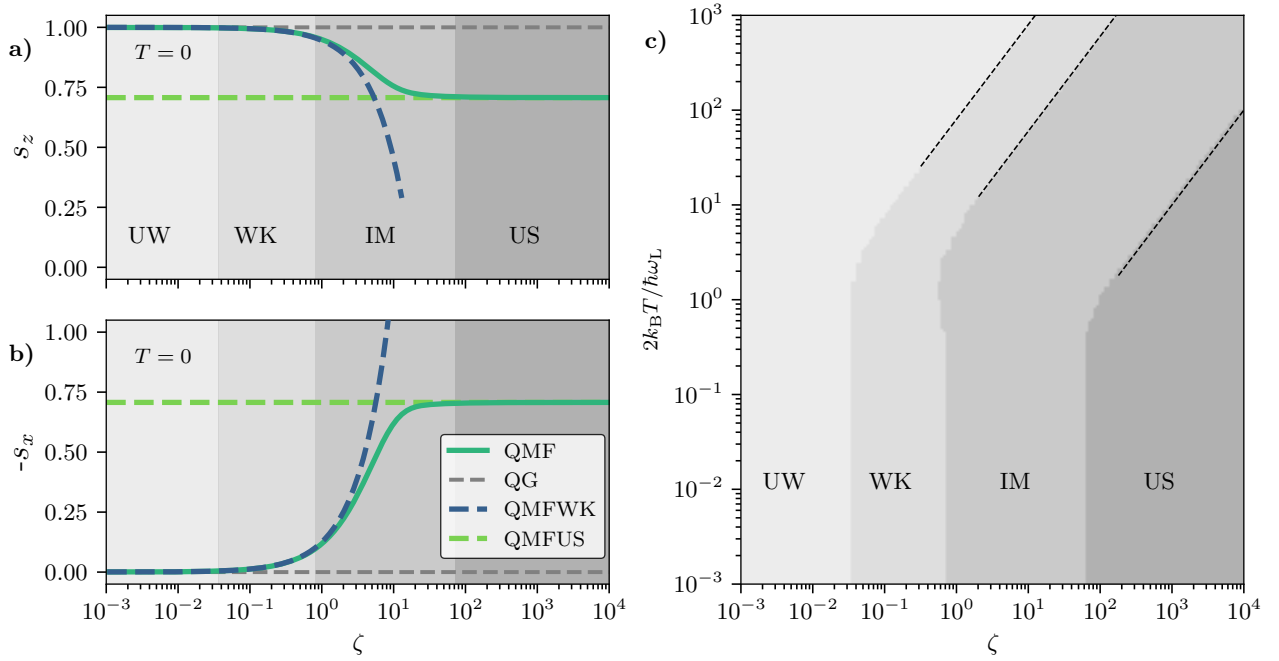


FIG. 6. **Coupling regimes.** **a)** and **b)**: Equilibrium spin expectation values s_z and $-s_x$ at $T = 0$ for $\theta = \pi/4$ and different coupling strengths as quantified by the dimensionless parameter ζ (see (10)). We identify four different regimes of coupling strength: (i) Ultraweak coupling (UW), where the spin expectation values are consistent with the Gibbs state (QG, dashed grey) of the bare Hamiltonian H_S ; (ii) Weak coupling (WK), where the expectation values are well approximated by a second order expansion in ζ (QMFWK, dashed blue) [34]; (iii) Intermediate coupling (IM), for which higher order corrections cannot be neglected (QMF, solid green); and (iv) Ultrastrong coupling (US), where the asymptotic limit of infinitely strong coupling $\zeta \rightarrow \infty$ is valid (QMFUS, dashed light green) [33]. **c)**: Identification of the four different coupling regimes UW, WK, IM, and US as a function of temperature T for $\theta = \pi/4$. With increasing temperature, the boundaries shift towards higher coupling ζ . At large temperatures, all three boundaries follow a linear relation $T \propto \zeta$ (dashed lines).

the scaling choice (8), one has $\zeta = \alpha$. It's important to note that temperature sets another scale in this problem – higher temperatures will allow higher coupling values ζ to still fall within the “weak” coupling regime [33, 65]. Thus, we will first characterise various coupling regimes at $T = 0$, where the coupling has the most significant effect on the system equilibrium state, and then proceed to study finite temperatures.

Fig. 6a) and 6b) show the spin components s_z and s_x in the quantum MF state (QMF, solid green). These expressions are evaluated numerically using the reaction coordinate method [66–69], see Supplement F. Also shown are the spin components for the quantum Gibbs state (QG, dashed grey), for the quantum MF state in the weak coupling limit (QMFWK, dashed blue), and for the quantum MF state in the ultrastrong coupling limit (QMFUS, dashed light green) [33]. Fig. 6a) and 6b) clearly show the transition from Gibbs state to mean force physics. The plots also allow us to identify four very different coupling regimes. The ultraweak (UW) limit, where the spin expectation values match those of the Gibbs state, is valid at very small coupling ($\zeta < 4 \cdot 10^{-2}$, first shaded area). For increasing ζ , one enters the well studied weak coupling regime (WK), where corrections to QG are important – in particular, one now has $s_x \neq 0$ – but still described by second order corrections in ζ [33]. This WK regime (second shaded

area) applies for reorganization energies satisfying

$$\text{WK: } Q \lesssim 0.8 \frac{\omega_L}{S_0}. \quad (11)$$

For larger ζ , condition (11) is no longer satisfied, and one crosses into the regime of intermediate coupling (IM, third shaded area). This regime is highly relevant from an experimental point of view but not yet well understood. Here we find very considerable deviations of the numerically exact quantum MF expressions (solid green) from those obtained with the weak coupling approximation (dashed blue). We also observe a turning point at ca. $\zeta = 10$ in the quantum MF plots of s_x and s_z (solid green). When increasing the coupling even further ($\zeta > 70$), s_z and s_x again become roughly independent of ζ , and converge to the known [33] ultrastrong coupling limit (QMFUS, dashed green). Thus, at $T = 0$, the ultrastrong regime applies for reorganisation energies satisfying (fourth shaded area)

$$\text{US: } Q > 70 \frac{\omega_L}{S_0}. \quad (12)$$

To illustrate the impact of temperature on the regime boundaries, we further compute s_x and s_z over a wide range of coupling strengths ($10^{-3} < \zeta < 10^4$) and temperatures ($10^{-3} < 2k_B T / \hbar \omega_L < 10^3$), and compare the results with those of the UW, WK, and US approximations. To determine if an approximation is good

enough, we require that the relative error compared to the exact quantum MF prediction must be less than $4 \cdot 10^{-3}$. Fig. 6c) shows the various coupling ranges as a function of ζ and T . One can see that, at elevated temperatures, the coupling regime boundaries shift towards higher coupling ζ . Thus at higher temperatures, $2k_B T / \hbar \omega_L \gtrsim 10$, the UW and WK approximations are valid at much higher coupling strengths ζ than at $T = 0$. At higher temperatures, we also observe an emerging linear relation, $2k_B T / \hbar \omega_L \propto \zeta$, for all three regime boundaries. The temperature dependence of the border between the weak and intermediate coupling regime has previously been identified to be linear by Latune [65]. This linear behaviour is indeed observed for $2k_B T > \hbar \omega_L$, while it breaks down at lower temperatures.

The above coupling regime results apply for a quantum spin. However, a similar analysis can be done for a classical spin and detailed plots analogous to that of Fig. 6 are shown in Supplement H. Surprisingly, we find that the classical regime boundary values of ζ significantly differ from those for the quantum spin, e.g. by a factor of 10 for the WK approximation. This implies that whether a particular coupling value ζ is “weak coupling” or not, depends on whether one considers a quantum spin or a classical spin. We suspect this discrepancy is related to the fact that, while for the classical case the entire dependence on the environment is contained in the reorganisation energy Q , the dependence on the environment spectral density is significantly more complex in the quantum case [70].

Discussion. We have characterised the equilibrium properties of the θ -angled spin boson model via the mean force Gibbs state approach. For the classical counterpart of this model, we found an analytical expression for τ_{MF} , valid at all coupling strengths. As a second result, we proved that the large-spin limit of the quantum MF state is precisely this classical MF state at all coupling strengths, provided that the coupling scales with the inverse square root of the spin length. Surprisingly, we further find that the environment-induced coherences, present in the quantum MF, persist for a classical spin whenever the environment interaction is anisotropic (i.e. $\theta \neq 0, \pi/2$). This implies that obser-

vation of a spin alignment that deviates from the bare spin Hamiltonian basis does not, by itself, provide sufficient evidence of quantum behaviour. While quantum coherences are known to be thermodynamically useful, for example for work extraction [61], classical inhomogeneities have only recently been identified to have a similar resource character [63]. It would be insightful to establish optimal classical protocols designed to extract work from classical inhomogeneous spin states, such as τ_{MF} shown in Fig. 4, and give a direct comparison of the work outputs of the classical and the quantum coherent case [63].

Finally, introducing a relative coupling parameter ζ , we identified four different coupling regimes, UW, WK, IM, US, and specified their range of validity. Importantly, the relevance of the different regimes is strongly temperature dependent, with weak coupling approximations being valid at larger ζ for higher temperatures. We further found that there are quantitative differences between the classical and quantum notions of “weak” and “strong” coupling.

Our results illustrate the classical nature of the coherences identified in spin systems that are anisotropically coupled to their environment, as well as the interplay between the quantum and mean force corrections to standard equilibrium states. This helps elucidate the quantum to classical boundary, which can find application in a wide range of fields, from magnetism to exciton dynamics. Finally, for a specific model choice, we showed that the mean force corrected classical state converges to the quantum Gibbs state. This opens the door to exploring the possibility of simulating some quantum behaviour by mimicking it with classical mean force behaviour that can be efficiently simulated [44].

Acknowledgments. We thank Anton Trushechkin for stimulating discussions on the subject of this research. FC gratefully acknowledges funding from the Foundational Questions Institute Fund (FQXi-IAF19-01). SS is supported by a DTP grant from EPSRC (EP/R513210/1). SARH acknowledges funding from the Royal Society and TATA (RPG-2016-186). JA, MB and JC gratefully acknowledge funding from EPSRC (EP/R045577/1). JA thanks the Royal Society for support.

-
- [1] N. Bohr, Über die serienspektren der elemente, *Zeitschrift für Physik* **2**, 423 (1920).
 - [2] K. Millard and H. S. Leff, Infinite-spin limit of the quantum heisenberg model, *Journal of Mathematical Physics* **12**, 1000 (1971).
 - [3] E. H. Lieb, The classical limit of quantum spin systems, *Communications in Mathematical Physics* **31**, 327 (1973).
 - [4] R. L. Liboff, Bohr correspondence principle for large quantum numbers, *Foundations of Physics* **5**, 271–293 (1975).
 - [5] R. L. Liboff, The correspondence principle revisited, *Physics Today* **37**, 50–55 (1984).
 - [6] M. Kryvohuz and J. Cao, Quantum-classical correspondence in response theory, *Phys. Rev. Lett.* **95**, 180405 (2005).
 - [7] E.-M. Graefe, H. J. Korsch, and A. E. Niederle, Quantum-classical correspondence for a non-hermitian bose-hubbard dimer, *Phys. Rev. A* **82**, 013629 (2010).
 - [8] C. Jarzynski, H. T. Quan, and S. Rahav, Quantum-classical correspondence principle for work distributions, *Phys. Rev. X* **5**, 031038 (2015).
 - [9] J.-F. Chen, T. Qiu, and H.-T. Quan, Quantum-classical correspondence principle for heat distribution in quantum brownian motion, *Entropy* **23**, 10.3390/e23121602 (2021).
 - [10] R. F. L. Evans, W. J. Fan, P. Chureemart, T. A. Ostler, M. O. A. Ellis, and R. W. Chantrell, Atomistic spin model simulations of magnetic nanomaterials, *Journal of Physics: Condensed Matter* **26**, 103202 (2014).

- [11] R. F. L. Evans, W. J. Fan, P. Chureemart, T. A. Ostler, M. O. A. Ellis, and R. W. Chantrell, Atomistic spin model simulations of magnetic nanomaterials, *Journal of Physics: Condensed Matter* **26**, 103202 (2014).
- [12] J. Barker and G. E. W. Bauer, Semiquantum thermodynamics of complex ferrimagnets, *Phys. Rev. B* **100**, 140401 (2019).
- [13] M. Strungaru, M. O. A. Ellis, S. Ruta, O. Chubykalo-Fesenko, R. F. L. Evans, and R. W. Chantrell, Spin-lattice dynamics model with angular momentum transfer for canonical and microcanonical ensembles, *Phys. Rev. B* **103**, 024429 (2021).
- [14] J. Barker and U. Atxitia, A review of modelling in ferrimagnetic spintronics, *Journal of the Physical Society of Japan* **90**, 081001 (2021).
- [15] P. Vorndamme, H.-J. Schmidt, C. Schröder, and J. Schnack, Observation of phase synchronization and alignment during free induction decay of quantum spins with heisenberg interactions, *New Journal of Physics* **23**, 083038 (2021).
- [16] C. Jarzynski, Nonequilibrium work theorem for a system strongly coupled to a thermal environment, *Journal of Statistical Mechanics: Theory and Experiment* **2004**, P09005 (2004).
- [17] U. Seifert, First and second law of thermodynamics at strong coupling, *Phys. Rev. Lett.* **116**, 020601 (2016).
- [18] C. Jarzynski, Stochastic and macroscopic thermodynamics of strongly coupled systems, *Phys. Rev. X* **7**, 011008 (2017).
- [19] P. Strasberg and M. Esposito, Stochastic thermodynamics in the strong coupling regime: An unambiguous approach based on coarse graining, *Phys. Rev. E* **95**, 062101 (2017).
- [20] H. J. D. Miller and J. Anders, Entropy production and time asymmetry in the presence of strong interactions, *Phys. Rev. E* **95**, 062123 (2017).
- [21] E. Aurell, Unified picture of strong-coupling stochastic thermodynamics and time reversals, *Phys. Rev. E* **97**, 042112 (2018).
- [22] T. Mori and S. Miyashita, Dynamics of the density matrix in contact with a thermal bath and the quantum master equation, *Journal of the Physical Society of Japan* **77**, 124005 (2008).
- [23] M. Campisi, P. Talkner, and P. Hänggi, Thermodynamics and fluctuation theorems for a strongly coupled open quantum system: an exactly solvable case, *Journal of Physics A: Mathematical and Theoretical* **42**, 392002 (2009).
- [24] S. Hilt, S. Shabbir, J. Anders, and E. Lutz, Landauer's principle in the quantum regime, *Phys. Rev. E* **83**, 030102 (2011).
- [25] C. H. Fleming and N. I. Cummings, Accuracy of perturbative master equations, *Physical Review E* **83**, 10.1103/physreve.83.031117 (2011).
- [26] J. Thingna, J.-S. Wang, and P. Hänggi, Generalized gibbs state with modified redfield solution: Exact agreement up to second order, *The Journal of Chemical Physics* **136**, 194110 (2012).
- [27] Y. Subaşı, C. H. Fleming, J. M. Taylor, and B. L. Hu, Equilibrium states of open quantum systems in the strong coupling regime, *Physical Review E* **86**, 10.1103/physreve.86.061132 (2012).
- [28] T. G. Philbin and J. Anders, Thermal energies of classical and quantum damped oscillators coupled to reservoirs, *Journal of Physics A: Mathematical and Theoretical* **49**, 215303 (2016).
- [29] H. J. D. Miller and J. Anders, Energy-temperature uncertainty relation in quantum thermodynamics, *Nature Communications* **9**, 10.1038/s41467-018-04536-7 (2018).
- [30] P. Strasberg, Repeated interactions and quantum stochastic thermodynamics at strong coupling, *Phys. Rev. Lett.* **123**, 180604 (2019).
- [31] A. Trushechkin, Quantum master equations and steady states for the ultrastrong-coupling limit and the strong-decoherence limit, *arXiv preprint arXiv:2109.01888* (2021), [arXiv:2109.01888](https://arxiv.org/abs/2109.01888).
- [32] A. S. Trushechkin, M. Merkli, J. D. Cresser, and J. Anders, Open quantum system dynamics and the mean force gibbs state, *AVS Quantum Science* **4**, 012301 (2022).
- [33] J. D. Cresser and J. Anders, Weak and ultrastrong coupling limits of the quantum mean force gibbs state, *Phys. Rev. Lett.* **127**, 250601 (2021).
- [34] A. Purkayastha, G. Guarnieri, M. T. Mitchison, R. Filip, and J. Goold, Tunable phonon-induced steady-state coherence in a double-quantum-dot charge qubit, *npj Quantum Information* **6**, 10.1038/s41534-020-0256-6 (2020).
- [35] L. Ferialdi, Exact non-markovian master equation for the spin-boson and jaynes-cummings models, *Phys. Rev. A* **95**, 020101 (2017).
- [36] Y.-F. Chiu, A. Strathearn, and J. Keeling, Numerical evaluation and robustness of the quantum mean force gibbs state, *arXiv preprint arXiv:2112.08254* (2021), [arXiv:2112.08254](https://arxiv.org/abs/2112.08254) [quant-ph].
- [37] A. Trushechkin, Calculation of coherences in förster and modified redfield theories of excitation energy transfer, *The Journal of Chemical Physics* **151**, 074101 (2019).
- [38] M. Yang and G. R. Fleming, Influence of phonons on exciton transfer dynamics: comparison of the redfield, förster, and modified redfield equations, *Chemical Physics* **282**, 163 (2002).
- [39] A. Koli, E. J. O'Reilly, G. D. Scholes, and A. Olaya-Castro, The fundamental role of quantized vibrations in coherent light harvesting by cryptophyte algae, *The Journal of Chemical Physics* **137**, 174109 (2012).
- [40] J. M. Moix, Y. Zhao, and J. Cao, Equilibrium-reduced density matrix formulation: Influence of noise, disorder, and temperature on localization in excitonic systems, *Phys. Rev. B* **85**, 115412 (2012).
- [41] S. Huelga and M. Plenio, Vibrations, quanta and biology, *Contemporary Physics* **54**, 181 (2013).
- [42] J. Seibt and T. Mančal, Ultrafast energy transfer with competing channels: Non-equilibrium förster and modified redfield theories, *The Journal of Chemical Physics* **146**, 174109 (2017).
- [43] A. Gelzinis and L. Valkunas, Analytical derivation of equilibrium state for open quantum system, *The Journal of Chemical Physics* **152**, 051103 (2020).
- [44] J. Anders, C. R. J. Sait, and S. A. R. Horsley, Quantum brownian motion for magnets, *New Journal of Physics* **24**, 033020 (2022).
- [45] A. Nazir, Correlation-dependent coherent to incoherent transitions in resonant energy transfer dynamics, *Phys. Rev. Lett.* **103**, 146404 (2009).
- [46] A. Recati, P. O. Fedichev, W. Zwerger, J. von Delft, and P. Zoller, Atomic quantum dots coupled to a reservoir of a superfluid bose-einstein condensate, *Phys. Rev. Lett.* **94**, 040404 (2005).
- [47] L. Magazzù, P. Forn-Díaz, R. Belyansky, J.-L. Orgiazzi, M. A. Yurtalan, M. R. Otto, A. Lupascu, C. M. Wilson, and M. Grifoni, Probing the strongly driven spin-boson model in a superconducting quantum circuit, *Nature Communications* **9**, 10.1038/s41467-018-03626-w (2018).

- [48] M. Popovic, M. T. Mitchison, A. Strathearn, B. W. Lovett, J. Goold, and P. R. Eastham, Quantum heat statistics with time-evolving matrix product operators, *PRX Quantum* **2**, 020338 (2021).
- [49] H.-P. Breuer and F. Petruccione, *The Theory of Open Quantum Systems* (Oxford University Press, 2007).
- [50] B. Huttner and S. M. Barnett, Quantization of the electromagnetic field in dielectrics, *Phys. Rev. A* **46**, 4306 (1992).
- [51] A. Fruchtmann, N. Lambert, and E. M. Gauger, When do perturbative approaches accurately capture the dynamics of complex quantum systems?, *Scientific Reports* **6**, 2045 (2016).
- [52] J. Wu, F. Liu, Y. Shen, J. Cao, and R. J. Silbey, Efficient energy transfer in light-harvesting systems, i: optimal temperature, reorganization energy and spatial-temporal correlations, *New Journal of Physics* **12**, 105012 (2010).
- [53] G. Ritschel, J. Roden, W. T. Strunz, and A. Eisfeld, An efficient method to calculate excitation energy transfer in light-harvesting systems: application to the fenna-matthews-olson complex, *New Journal of Physics* **13**, 113034 (2011).
- [54] C. L. Latune, Steady state in ultrastrong coupling regime: perturbative expansion and first orders, arXiv preprint [arXiv:2110.02186](https://arxiv.org/abs/2110.02186) (2021), [arXiv:2110.02186](https://arxiv.org/abs/2110.02186) [quant-ph].
- [55] See later discussions where the different regimes of coupling strength are thoroughly characterised.
- [56] To see this, note that simply increasing S_0 in (6) would have the same effect as sending $\beta \rightarrow \infty$; namely, all population will go to the ground state.
- [57] M. E. Fisher, Magnetism in one-dimensional systems—the heisenberg model for infinite spin, *American Journal of Physics* **32**, 343 (1964).
- [58] Note that for a fixed value of S_0 , the factor of $\frac{\hbar}{2S_0+\hbar}$ is un-important as it immediately cancels in any calculation of expectation values, i.e. for a quantum system, the expressions $\frac{\hbar}{2S_0+\hbar} Z_S^{\text{qu}}(\beta, S_0)$ and $Z_S^{\text{qu}}(\beta, S_0)$ give the same expectation values.
- [59] S. Nemati, C. Henkel, and J. Anders, Coupling function from bath density of states, arXiv preprint [arXiv:2112.04001](https://arxiv.org/abs/2112.04001) (2021), [2112.04001](https://arxiv.org/abs/2112.04001) [quant-ph].
- [60] G. Guarnieri, M. Kolář, and R. Filip, Steady-state coherences by composite system-bath interactions, *Phys. Rev. Lett.* **121**, 070401 (2018).
- [61] P. Kammerlander and J. Anders, Coherence and measurement in quantum thermodynamics, *Scientific Reports* **6**, 10.1038/srep22174 (2016).
- [62] H.-H. Hasegawa, J. Ishikawa, K. Takara, and D. Driebe, Generalization of the second law for a nonequilibrium initial state, *Physics Letters A* **374**, 1001 (2010).
- [63] A. Smith, K. Sinha, and C. Jarzynski, Quantum coherences and classical inhomogeneities as equivalent thermodynamics resources, *Entropy* **24**, 10.3390/e24040474 (2022).
- [64] Strictly speaking, for $\theta = 0$ the full Hamiltonian's eigenstates are product states of the spin and environment. Thus, no energy transfer can occur between them, and the system would not be able to equilibrate. Here, we will understand $\theta = 0$ as a limiting case of the coupling angle θ to be infinitesimally small, but not strictly zero, so as to ensure that there is dissipation.
- [65] C. L. Latune, Steady state in strong system-bath coupling regime: Reaction coordinate versus perturbative expansion, *Phys. Rev. E* **105**, 024126 (2022).
- [66] J. Iles-Smith, N. Lambert, and A. Nazir, Environmental dynamics, correlations, and the emergence of non-canonical equilibrium states in open quantum systems, *Phys. Rev. A* **90**, 032114 (2014).
- [67] J. Iles-Smith, A. G. Dijkstra, N. Lambert, and A. Nazir, Energy transfer in structured and unstructured environments: Master equations beyond the born-markov approximations, *The Journal of Chemical Physics* **144**, 044110 (2016).
- [68] A. Nazir and G. Schaller, The reaction coordinate mapping in quantum thermodynamics, in *Thermodynamics in the Quantum Regime: Fundamental Aspects and New Directions*, edited by F. Binder, L. A. Correa, C. Gogolin, J. Anders, and G. Adesso (Springer International Publishing, Cham, 2018) pp. 551–577.
- [69] L. A. Correa, B. Xu, B. Morris, and G. Adesso, Pushing the limits of the reaction-coordinate mapping, *The Journal of Chemical Physics* **151**, 094107 (2019).
- [70] J. Anders and K. Wiesner, Increasing complexity with quantum physics, *Chaos: An Interdisciplinary Journal of Nonlinear Science* **21**, 037102 (2011).
- [71] A. Lemmer, C. Cormick, D. Tamascelli, T. Schaetz, S. F. Huelga, and M. B. Plenio, A trapped-ion simulator for spin-boson models with structured environments, *New Journal of Physics* **20**, 073002 (2018).
- [72] N. Lambert, S. Ahmed, M. Cirio, and F. Nori, Modelling the ultra-strongly coupled spin-boson model with unphysical modes, *Nature Communications* **10**, 3721 (2019).
- [73] Y. K. Wang and F. T. Hioe, Phase transition in the dicke model of superradiance, *Phys. Rev. A* **7**, 831 (1973).
- [74] M. Campisi, P. Talkner, and P. Hänggi, Fluctuation theorem for arbitrary open quantum systems, *Phys. Rev. Lett.* **102**, 210401 (2009).
- [75] P. Strasberg and M. Esposito, Measurability of nonequilibrium thermodynamics in terms of the hamiltonian of mean force, *Phys. Rev. E* **101**, 050101 (2020).

Appendix A: Tracing for spin and reservoir, in classical and quantum setting

1. Spin tracing in the classical setting

For a classical spin of length S_0 , with components S_x, S_y, S_z , one can change into spherical coordinates, i.e.

$$S_x = S_0 \sin \vartheta \cos \varphi, \quad S_y = S_0 \sin \vartheta \sin \varphi, \quad S_z = S_0 \cos \vartheta, \quad \vartheta \in [0, \pi], \varphi \in [0, 2\pi]. \quad (\text{A1})$$

Then, traces of functions $A(S_x, S_z)$ are evaluated as

$$\text{tr}_S^{\text{cl}}[A(S_x, S_z)] = \frac{1}{4\pi} \int_0^{2\pi} d\varphi \int_0^\pi d\vartheta \sin \vartheta A(S_0 \sin \vartheta \cos \varphi, S_0 \cos \vartheta). \quad (\text{A2})$$

2. Spin tracing in the quantum setting

For a quantum spin S_0 , given any orthogonal basis $|m\rangle$, then the trace of functions of the spin operators $A(S_x, S_z)$ are evaluated as

$$\text{tr}_S^{\text{qu}}[A(S_x, S_z)] = \sum_m \langle m | A(S_x, S_z) | m \rangle. \quad (\text{A3})$$

Given that the trace is independent of the choice of basis, the basis $|m\rangle$ is typically chosen as is more convenient to perform the calculation depending on the specific form of the operator $A(S_x, S_z)$.

3. Reservoir traces

When taking traces over the environmental degrees of freedom (in either the classical or quantum case), we ought to first discretise the energy spectrum of H_R . This is because, strictly speaking, the partition function for the reservoir, $Z_R = \text{tr}[\exp(-\beta H_R)]$, is not well defined in the continuum limit. Thus, we write

$$H_R = \sum_{n=0}^{\infty} \frac{1}{2} (P_{\omega_n}^2 + \omega_n^2 X_{\omega_n}^2). \quad (\text{A4})$$

Then, for example, the classical partition function of the environment is

$$Z_R^{\text{cl}} = \prod_n \int_{-\infty}^{+\infty} dX_{\omega_n} \int_{-\infty}^{\infty} dP_{\omega_n} \exp \left[-\frac{1}{2} \beta \left(P_{\omega_n}^2 + \omega_n^2 \left(X_{\omega_n} - \frac{S_\theta C_{\omega_n}}{\omega_n^2} \right)^2 \right) \right], \quad (\text{A5})$$

and similarly for the quantum case.

Appendix B: Expectation values from the partition function

With the partition function of the MF we can proceed to calculate the S_z and S_x expectation values as follows.

1. Classical case

For the classical spin, from (7) we have the partition function

$$\tilde{Z}_S^{\text{cl}} = \frac{1}{4\pi} \int_0^{2\pi} d\varphi \int_0^\pi d\vartheta \sin \vartheta e^{-\beta(-\omega_L S_z(\vartheta, \phi) - Q S_\theta^2(\vartheta, \phi))}. \quad (\text{B1})$$

While obtaining the S_z expectation value is straightforward, the S_x case may seem less obvious. It is therefore convenient to do a change of coordinates

$$S_{z'} = S_z \cos \theta - S_x \sin \theta, \quad S_{x'} = S_x \cos \theta + S_z \sin \theta, \quad (\text{B2})$$

so that

$$\tilde{Z}_S^{\text{cl}} = \frac{1}{4\pi} \int_0^{2\pi} d\varphi \int_0^\pi d\vartheta \sin \vartheta e^{-\beta(-\omega_L \cos \theta S_{z'}(\vartheta, \phi) - \omega_L \sin \theta S_{x'}(\vartheta, \phi) - Q S_{z'}^2(\vartheta, \phi))}. \quad (\text{B3})$$

Now defining $h_{x'} = -\omega_L \sin \theta$, $h_{z'} = -\omega_L \cos \theta$, we have that

$$\tilde{Z}_S^{\text{cl}} = \frac{1}{4\pi} \int_0^{2\pi} d\varphi \int_0^\pi d\vartheta \sin \vartheta e^{-\beta(h_{z'} S_{z'}(\vartheta, \phi) + h_{x'} S_{x'}(\vartheta, \phi) - Q S_{z'}^2(\vartheta, \phi))}, \quad (\text{B4})$$

and we can obtain the $S_{z'}$ and $S_{x'}$ expectation values as usual, i.e.

$$\langle S_{x', z'} \rangle = -\frac{1}{\beta} \frac{\partial}{\partial h_{x', z'}} \log \tilde{Z}_S^{\text{cl}}. \quad (\text{B5})$$

Finally, by linearity, we have that

$$\langle S_x \rangle = \langle S_{x'} \rangle \cos \theta - \langle S_{z'} \rangle \sin \theta, \quad \langle S_z \rangle = \langle S_{z'} \rangle \cos \theta + \langle S_{x'} \rangle \sin \theta. \quad (\text{B6})$$

2. Quantum case

For the quantum case we proceed in a completely analogous manner. We have that

$$\langle S_x \rangle = \text{tr}^{\text{qu}} \left[S_x e^{-\beta(-\omega_L S_z + S_\theta B + H_R)} \right], \quad \langle S_z \rangle = \text{tr}^{\text{qu}} \left[S_z e^{-\beta(-\omega_L S_z + S_\theta B + H_R)} \right]. \quad (\text{B7})$$

Starting from the partition function

$$Z_{\text{SR}}^{\text{qu}} = \text{tr}^{\text{qu}} \left[e^{-\beta(-\omega_L S_z + S_\theta B + H_R)} \right], \quad (\text{B8})$$

we define a new set of rotated operators,

$$S_{z'} = S_z \cos \theta - S_x \sin \theta, \quad S_{x'} = S_x \cos \theta + S_z \sin \theta, \quad (\text{B9})$$

and variables $h_{x'} = -\omega_L \sin \theta$, $h_{z'} = -\omega_L \cos \theta$, so that

$$Z_{\text{SR}}^{\text{qu}} = \text{tr}^{\text{qu}} [e^{-\beta(h_{z'} S_{z'} + h_{x'} S_{x'} + S_{z'} B + H_R)}]. \quad (\text{B10})$$

Then, the expectation values of the new operators $S_{x'}, S_{z'}$ can be obtained as

$$\langle S_{x', z'} \rangle = -\frac{1}{\beta} \frac{\partial}{\partial h_{x', z'}} \log Z_{\text{SR}}^{\text{qu}}. \quad (\text{B11})$$

Finally, $\langle S_x \rangle$ and $\langle S_z \rangle$ follow from linearity

$$\langle S_x \rangle = \langle S_{x'} \rangle \cos \theta - \langle S_{z'} \rangle \sin \theta, \quad \langle S_z \rangle = \langle S_{z'} \rangle \cos \theta + \langle S_{x'} \rangle \sin \theta. \quad (\text{B12})$$

3. Example: Ultrastrong limit

Let us consider the ultrastrong partition function (either quantum or classical since they coincide),

$$\tilde{Z}_{\text{S,US}} = \cosh(\beta \omega_L S_0 \cos \theta). \quad (\text{B13})$$

Following the procedure outlined above, we have that $h_{z'} = -\omega_L \cos \theta$, and therefore

$$\tilde{Z}_{\text{S,US}} = \cosh(\beta S_0 h_{z'}). \quad (\text{B14})$$

Therefore, the expectation values of the transformed observables are

$$\langle S_{x'} \rangle = -\frac{1}{\beta} \frac{\partial}{\partial h_{x'}} \log \tilde{Z}_{\text{S,US}} = 0, \quad (\text{B15})$$

$$\langle S_{z'} \rangle = -\frac{1}{\beta} \frac{\partial}{\partial h_{z'}} \log \tilde{Z}_{\text{S,US}} = -S_0 \tanh(\beta S_0 h_{z'}) = -S_0 \tanh(\beta \omega_L S_0 \cos \theta). \quad (\text{B16})$$

Therefore, in the original variables we have

$$\langle S_x \rangle = \langle S_{x'} \rangle \cos \theta - \langle S_{z'} \rangle \sin \theta = S_0 \sin \theta \tanh(\beta \omega_L S_0 \cos \theta), \quad (\text{B17})$$

$$\langle S_z \rangle = \langle S_{z'} \rangle \cos \theta + \langle S_{x'} \rangle \sin \theta = -S_0 \cos \theta \tanh(\beta \omega_L S_0 \cos \theta), \quad (\text{B18})$$

in agreement with what is later obtained directly from the MF in the ultra-strong limit.

Appendix C: Derivation of classical MF for arbitrary coupling

In this section we derive the mean force Gibbs state of the classical spin for arbitrary coupling strength. As discussed in A, we discretise the environmental degrees of freedom, and thus we have for the total Hamiltonian, (3)

$$H_{\text{tot}} = -\omega_L S_z + \sum_{n=0}^{\infty} \left[\frac{1}{2} (P_{\omega_n}^2 + \omega_n^2 X_{\omega_n}^2) - S_{\theta} C_{\omega_n} X_{\omega_n} \right]. \quad (\text{C1})$$

On 'completing the square', we get

$$H_{\text{tot}} = -\omega_L S_z + \sum_{n=0}^{\infty} \left[\frac{1}{2} \left[P_{\omega_n}^2 + \omega_n^2 \left(X_{\omega_n} - \frac{S_{\theta} C_{\omega_n}}{\omega_n^2} \right)^2 \right] - \frac{(S_{\theta} C_{\omega_n})^2}{2\omega_n^2} \right]. \quad (\text{C2})$$

The partition function is then,

$$Z_{\text{SR}}^{\text{cl}} = \int_0^{2\pi} d\varphi \int_0^{\pi} d\vartheta \sin \vartheta \exp[-\beta H_{\text{eff}}] Z_{\text{R}}^{\text{cl}}. \quad (\text{C3})$$

Here,

$$Z_{\text{R}}^{\text{cl}} = \prod_n \int_{-\infty}^{\infty} dX_{\omega_n} \int_{-\infty}^{\infty} dP_{\omega_n} \exp \left[-\frac{1}{2} \beta \left(P_{\omega_n}^2 + \omega_n^2 \left(X_{\omega_n} - \frac{S_{\theta} C_{\omega_n}}{\omega_n^2} \right)^2 \right) \right], \quad (\text{C4})$$

is the partition function for the reservoir only, and there appears an effective system Hamiltonian given by

$$H_{\text{eff}} \equiv -\omega_L S_z - Q S_{\theta}^2 \quad (\text{C5})$$

where the reorganization energy Q , is given by Eq. (5) of the main text.

While it is possible to derive an expression for Z_{R} , its details are not needed as it depends solely on reservoir variables and can be divided out to yield the partition function of the system's MF,

$$\tilde{Z}_{\text{S}}^{\text{cl}} = \frac{Z_{\text{SR}}^{\text{cl}}}{Z_{\text{R}}^{\text{cl}}} = \int_0^{2\pi} d\varphi \int_0^{\pi} d\vartheta \sin \vartheta \exp[-\beta H_{\text{eff}}], \quad (\text{C6})$$

where H_{eff} includes all spin terms independent of the coordinates of the environment. Finally, the MF is given by

$$\tau_{\text{MF}} = \frac{1}{\tilde{Z}_{\text{S}}^{\text{cl}}} \exp[-\beta H_{\text{eff}}], \quad (\text{C7})$$

which is precisely Eq. (7) of the main text.

In terms of polar coordinates, we have $S_z = S_0 \cos \vartheta$ and $S_x = S_0 \cos \varphi \sin \vartheta$. Therefore, $S_{\theta} = S_0 (\cos \vartheta \cos \theta - \sin \vartheta \cos \varphi \sin \theta)$, and we have that

$$H_{\text{eff}}(\vartheta, \varphi) = -\omega_L S_0 \cos \vartheta - S_0^2 Q (\cos \theta \cos \vartheta - \sin \theta \sin \vartheta \cos \varphi)^2. \quad (\text{C8})$$

The equilibrium state of the spin is then entirely determined by $\tilde{Z}_{\text{S}}^{\text{cl}}$. The classical expectation values for the spin components S_z and S_x are then given by

$$\langle s_z \rangle = \frac{\langle S_z \rangle}{S_0} = \frac{1}{\tilde{Z}_{\text{S}}^{\text{cl}}} \int_0^{2\pi} d\varphi \int_0^{\pi} d\vartheta \sin \vartheta \cos \vartheta \exp[-\beta H_{\text{eff}}(\vartheta, \varphi)] \quad (\text{C9})$$

$$\langle s_x \rangle = \frac{\langle S_x \rangle}{S_0} = \frac{1}{\tilde{Z}_{\text{S}}^{\text{cl}}} \int_0^{2\pi} d\varphi \cos \varphi \int_0^{\pi} d\vartheta \sin^2 \vartheta \exp[-\beta H_{\text{eff}}(\vartheta, \varphi)]. \quad (\text{C10})$$

The integral expressions for the expectation values above cannot in general be expressed in a closed form, but can be readily evaluated numerically for arbitrary coupling strength Q .

Appendix D: Dynamical steady state and MF state for a classical spin.

Throughout this article, we have assumed that the MF is the equilibrium state reached by a system in contact with a thermal bath. While this is widely thought to be the case, some open questions remain about formal proofs showing the convergence of the dynamics towards the steady state predicted by the MF state [32]. For example,

for quantum systems, this convergence has only been proven in the weak [22] and ultrastrong limits [31], while for intermediate coupling strengths there is numerical evidence for the validity of the MF state [36]. Here we proceed to numerically verify the convergence of the dynamics towards the MF state for the case of the classical spin at arbitrary coupling strength. This is possible thanks to the numerical method proposed in [44]. Solving the dynamics for general coupling C_ω can be very challenging, given that the reservoir interaction induces memory effects. However, the complexity of the problem drastically simplifies if we choose a Lorentzian spectral density [44, 71], given by

$$J_\omega = \frac{A\Gamma}{\pi} \frac{\omega}{(\omega_0^2 - \omega^2)^2 + \Gamma^2\omega^2}, \quad (\text{D1})$$

where ω_0 is the resonant frequency of the Lorentzian and Γ the peak width. The parameter A regulates the strength of the spin–reservoir coupling, and will determine the coupling regime. This spectral density is sometimes referred to as an “underdamped spectrum” [67–69, 72] and is used to model coupling that is resonant in a specific range of frequencies and possesses a natural high frequency cutoff provided by the finite width Γ . Single Lorentzian couplings, or indeed multiple Lorentzians, represent physically realistic reservoir interactions [59, 71], while also being analytically and numerically tractable [44]. For the Lorentzian (D1), the reorganization energy (5) is $Q = A/(2\omega_0^2)$. One key practical advantage of the Lorentzian spectral density is that, as shown in [44], the equations of motion of the spin can be reduced into a set of ordinary differential equations that produce the exact dynamics for arbitrary coupling strength.

Fig. 2 shows the long time average of the spin components once the dynamics has reached steady state (CSS, triangles), together with the expectation values predicted by the static MF state (CMF, solid lines), for a wide range of coupling strengths going from weak to strong coupling. We find that both predictions are in excellent agreement, providing strong evidence for the convergence of the dynamics towards the MF.

Appendix E: Quantum-classical correspondence for the MF partition functions

The aim here is to determine the classical limit by taking the large spin limit, i.e., the limit of large S_0 for the θ -spin-boson model. This will be done along the lines of the method due to Fisher, Millard & Leff, and Lieb [2, 3, 57], extended to take into account the presence of the interaction of the system with a reservoir. The total Hamiltonian is (3) and, as discussed in the main text, the coupling C_ω in (4) is chosen to scale with S_0 as $C_\omega \propto 1/\sqrt{S_0}$ and hence $J_\omega \propto 1/S_0$. The (unnormalised) global quantum Gibbs state is

$$e^{-\beta H_{\text{tot}}} = \exp[-\beta(-\omega_L S_z + H_R + S_\theta B)], \quad (\text{E1})$$

where $S_\theta = S_z \cos \theta - S_x \sin \theta$ and

$$B = \int_0^\infty d\omega C_\omega X_\omega. \quad (\text{E2})$$

We are seeking the large spin limit, $S_0 \rightarrow \infty$, of the corresponding quantum partition function

$$Z_{\text{SR}}^{\text{qu}}(\beta, S_0) = \text{tr}_{\text{SR}}^{\text{qu}}[\exp[-\beta(-\omega_L S_z + H_R + S_\theta B)]]. \quad (\text{E3})$$

1. Fisher rescaling and the Millard-Leff-Lieb identity

Taking the large spin limit for a spin- S_0 system can be achieved by an approach discussed by Fisher [57]. It involves introducing a rescaling of the spin operators via

$$s_i = \frac{S_i}{S_0}, \quad i = x, y, z. \quad (\text{E4})$$

Then, the usual commutation rule $[S_i, S_j] = i\hbar\epsilon_{ijk}S_k$ becomes $[s_i, s_j] = i\hbar\epsilon_{ijk}s_k/S_0$. Hence, in the limit of $S_0 \rightarrow \infty$, the scaled operators will commute so in that regard they can be considered as classical quantities. Fisher then proceeds to treat them as such, but a more rigorous result is found by Millard & Leff and Lieb [2, 3] who show that, taking this limit the replacements (cf. (A1))

$$s_x \rightarrow \sin \vartheta \cos \varphi, \quad s_y \rightarrow \sin \vartheta \sin \varphi, \quad s_z \rightarrow \cos \vartheta \quad (\text{E5})$$

can be made. For a system Hamiltonian H_S they prove the identity

$$\begin{aligned} & \lim_{S_0 \rightarrow \infty} \frac{\hbar}{2S_0 + \hbar} \text{tr}_S^{\text{qu}} \left[e^{-\beta H_S(S_x, S_y, S_z)} \right] \\ &= \lim_{S_0 \rightarrow \infty} \frac{1}{4\pi} \int_0^{2\pi} d\varphi \int_0^\pi d\vartheta \sin \vartheta e^{-\beta H_S(S_0 \sin \vartheta \cos \varphi, S_0 \sin \vartheta \sin \varphi, S_0 \cos \vartheta)}, \end{aligned} \quad (\text{E6})$$

provided the limit on the right hand side exists. This result is also proved by Lieb [3] who makes use of the properties of spin coherent states. Note, that the factor of $\frac{\hbar}{2S_0 + \hbar}$ is required to cancel the factor arising from the quantum trace over a multi-dimensional Hilbert space. I.e. setting $\beta = 0$ on both sides, the RHS will give 1, while the LHS would give $\frac{2S_0 + \hbar}{\hbar}$ without the inclusion of the factor.

We here take expression (E6) to be valid also for operators H_{tot} acting on the tensor product space of spin and reservoir degrees of freedom. We leave a mathematically rigorous proof of such generalisation for future work. Exemplar justification will be provided in Supplement I, showing the convergence of explicitly known quantum results (valid in the weak coupling regime) to the corresponding classical results.

The problem is to carry out the limit on the RHS of Eq. (E6). Since the system of interest is now coupled to a reservoir, a trace over the reservoir will also be required. As we will see below, this will imply a rescaling of the reservoir operators. One approach is to absorb the S_0 dependence into the parameters of the Hamiltonian H_{tot} . This is the approach of Fisher and others, so defines the ‘Fisher limit’. This limit requires a rescaling of the physical parameters of the Hamiltonian. A second approach is to rescale the temperature and take the limit $S_0 \rightarrow \infty$ with $\beta S_0 = \beta'$ held fixed. This is the limit we take here. Thus we wish to evaluate

$$\lim_{S_0 \rightarrow \infty} \frac{\hbar}{2S_0 + \hbar} Z_{\text{SR}}^{\text{qu}}(\beta, S_0) = \lim_{S_0 \rightarrow \infty} \frac{\hbar}{2S_0 + \hbar} \text{tr}_{\text{SR}}^{\text{qu}} \left[e^{-\beta H_{\text{tot}}(S_x, S_y, S_z)} \right] \quad \text{with } \beta = \beta'/S_0 \text{ and } \beta' \text{ constant.} \quad (\text{E7})$$

2. The $S_0 \rightarrow \infty$ limit of the quantum system-reservoir partition function $Z_{\text{SR}}^{\text{qu}}$

We write the unnormalised global Gibbs state as

$$e^{-\beta H_{\text{tot}}} = \exp \left[-\beta' \left(-\omega_L s_z + \frac{H_R}{S_0} + s_\theta \int_0^\infty d\omega C_\omega X_\omega \right) \right]. \quad (\text{E8})$$

with the rescaled inverse temperature $\beta' = \beta S_0$. β' is constant as the limit $S_0 \rightarrow \infty$ is taken and doing so rescales the spin operators, as required. But it also rescales H_R to H_R/S_0 , which can be expressed in terms of rescaled reservoir operators, i.e.,

$$h_R = \frac{H_R}{S_0} = \frac{1}{2} \int_0^\infty d\omega (p_\omega^2 + \omega^2 x_\omega^2), \quad (\text{E9})$$

where

$$p_\omega = \frac{P_\omega}{\sqrt{S_0}}, \quad x_\omega = \frac{X_\omega}{\sqrt{S_0}}. \quad (\text{E10})$$

We now find the commutation relation $[X_\omega, P_{\omega'}] = i\hbar\delta(\omega - \omega')$ becomes

$$[x_\omega, p_{\omega'}] = \frac{1}{S_0} i\hbar\delta(\omega - \omega'), \quad (\text{E11})$$

so in the limit of $S_0 \rightarrow \infty$, these two operators commute, and hence in a manner analogous to the spin operators, can be treated classically in this limit. This was also shown by Wang and Hioe [73], though their scaling was in the context of taking the limit $N \rightarrow \infty$ for N two-level atoms in the Dicke model.

Note that as a consequence of taking this limit, the quantum nature of the reservoir is inevitably stripped away, so that the result eventually obtained is that of a classical spin coupled to a classical reservoir. Written in terms of these operators, we have

$$e^{-\beta H_{\text{tot}}} = \exp \left[-\beta' \left(-\omega_L s_z + h_R + s_\theta \int_0^\infty d\omega C_\omega \sqrt{S_0} x_\omega \right) \right]. \quad (\text{E12})$$

Note that, by virtue of our choice of scaling $C_\omega \propto 1/\sqrt{S_0}$, the interaction term is independent of S_0 . We now “complete the square” for the combination

$$h_R + s_\theta \int_0^\infty d\omega C_\omega \sqrt{S_0} x_\omega, \quad (\text{E13})$$

to arrive at

$$\frac{1}{2} \int_0^\infty d\omega \left(p_\omega^2 + \omega^2 \left(x_\omega + s_\theta \frac{C_\omega \sqrt{S_0}}{\omega^2} \right)^2 \right) - s_\theta^2 S_0 Q(S_0) = h_R^{\text{shift}} - s_\theta^2 S_0 Q(S_0), \quad (\text{E14})$$

where $Q(S_0) = \int_0^\infty d\omega \frac{C_\omega^2(S_0)}{2\omega^2}$ is the reorganisation energy, see (5). Note that because of the scaling $C_\omega \propto 1/\sqrt{S_0}$, the product $S_0 Q(S_0)$ is independent of S_0 . Here we have defined the reservoir Hamiltonian

$$h_R^{\text{shift}} = \frac{1}{2} \int_0^\infty d\omega \left(p_\omega^2 + \omega^2 \left(x_\omega + s_\theta \frac{C_\omega \sqrt{S_0}}{\omega^2} \right)^2 \right), \quad (\text{E15})$$

where the oscillator centres have been shifted.

Extending the result (E6) proven by Millard & Leff and by Lieb to the spin-reservoir Hamiltonian H_{tot} , and immediately taking the reservoir trace on both sides, gives

$$\begin{aligned} \lim_{S_0 \rightarrow \infty} \frac{\hbar}{2S_0 + \hbar} Z_{\text{SR}}^{\text{qu}}(\beta, S_0) &= \\ &= \lim_{S_0 \rightarrow \infty} \frac{\hbar}{2S_0 + \hbar} \text{tr}_{\text{SR}}^{\text{qu}} \left[\exp \left[-\beta' \left(-\omega_L s_z + h_R^{\text{shift}} - s_\theta^2 S_0 Q(S_0) \right) \right] \right] \\ &= \lim_{S_0 \rightarrow \infty} \frac{1}{4\pi} \int_0^{2\pi} d\varphi \int_0^\pi d\vartheta \sin \vartheta \text{tr}_R \left[\exp \left[-\beta' \left(-\omega_L \cos \vartheta + h_R^{\text{shift}} - s_\theta^2(\vartheta, \phi') S_0 Q(S_0) \right) \right] \right] \\ &= \lim_{S_0 \rightarrow \infty} \frac{1}{4\pi} \int_0^{2\pi} d\varphi \int_0^\pi d\vartheta \sin \vartheta \exp \left[-\beta' \left(-\omega_L \cos \vartheta - s_\theta^2(\vartheta, \phi') S_0 Q(S_0) \right) \right] \text{tr}_R^{\text{qu}} \left[\exp \left(-\beta' h_R^{\text{shift}} \right) \right], \end{aligned} \quad (\text{E16})$$

where the trace over the reservoir now factors out and

$$s_\theta(\vartheta, \phi') = \cos \theta \cos \vartheta - \sin \theta \cos \varphi \sin \vartheta. \quad (\text{E17})$$

The reservoir trace factor gives

$$\text{tr}_R^{\text{qu}} \left[\exp \left[-\beta' h_R^{\text{shift}} \right] \right] = \text{tr}_R^{\text{qu}} \left[\exp \left[-\beta' \frac{1}{2} \int_0^\infty d\omega \left(P_\omega^2 + \omega^2 (X_\omega + \mu_\omega)^2 \right) \right] \right] = Z_R^{\text{qu}}(\beta), \quad (\text{E18})$$

with $\mu_\omega = S_\theta \frac{C_\omega}{\omega^2}$ a shift in the centre position of the oscillators. The operators $X_\omega + \mu_\omega$ have the same commutation relations with the P_ω as the X_ω themselves. Thus such a shift does not affect the trace and the result is the bare quantum reservoir partition function at inverse temperature β , i.e. $Z_R^{\text{qu}}(\beta)$.

Dividing by $Z_R^{\text{qu}}(\beta)$ on both sides, putting it all together, we find

$$\lim_{S_0 \rightarrow \infty} \frac{\hbar}{2S_0 + \hbar} \frac{Z_{\text{SR}}^{\text{qu}}(\beta, S_0)}{Z_R^{\text{qu}}(\beta)} = \frac{1}{4\pi} \int_0^{2\pi} d\varphi \int_0^\pi d\vartheta \sin \vartheta \exp \left[-\beta' \left(-\omega_L \cos \vartheta - s_\theta^2(\vartheta, \phi') S_0 Q(S_0) \right) \right]. \quad (\text{E19})$$

where we have dropped the limit symbol since there is no dependence on S_0 (recall that $S_0 Q(S_0)$ is independent of S_0).

Now we may replace again $\beta' = \beta S_0$, and the RHS emerges as the spin's classical mean force partition function $\tilde{Z}_S^{\text{cl}}(\beta S_0)$ cf. (7), where the classical trace is taken according to (A2). Moreover, the fraction of total quantum partition function divided by bare reservoir partition function is the quantum mean force partition function [74, 75]. Thus we conclude:

$$\lim_{S_0 \rightarrow \infty} \frac{\hbar}{2S_0 + \hbar} \tilde{Z}_S^{\text{qu}}(\beta, S_0) = \lim_{S_0 \rightarrow \infty} \frac{\hbar}{2S_0 + \hbar} \frac{Z_{\text{SR}}^{\text{qu}}(\beta, S_0)}{Z_R^{\text{qu}}(\beta)} = \tilde{Z}_S^{\text{cl}}(\beta S_0). \quad (\text{E20})$$

Appendix F: Quantum Reaction Coordinate mapping

The Reaction Coordinate mapping method [66–69] is a technique for dealing with systems strongly coupled to bosonic environments. To do so, it isolates a single collective environmental degree of freedom, the so called “reaction coordinate” (RC), that interacts with the system via an effective Hamiltonian. The rest of the environmental degrees of freedom manifest as a new bosonic environment coupled to the RC. Concretely, for our total Hamiltonian (3), the effective Hamiltonian that we have to consider is

$$H_{\text{tot}}^{\text{RC}} = H_S + H_{\text{RC}} + H_{\text{int}}^{\text{RC}} + H_{\text{int}}^{\text{res}} + H_{\text{res}}, \quad (\text{F1})$$

where H_{RC} is the Hamiltonian of the RC mode,

$$H_{\text{RC}} = \hbar \Omega_{\text{RC}} a^\dagger a, \quad (\text{F2})$$

with a^\dagger the creation operator of a quantum harmonic oscillator of frequency Ω_{RC} ; $H_{\text{int}}^{\text{RC}}$ is the spin-RC interaction

$$H_{\text{int}}^{\text{RC}} = \lambda_{\text{RC}} S_\theta (a + a^\dagger), \quad (\text{F3})$$

where λ_{RC} determines the coupling strength between the RC mode and the spin; $H_{\text{res}} = \int d\omega (p_\omega^2 + \omega^2 x_\omega^2)/2$ is the Hamiltonian of the residual bosonic bath; and finally the residual bath-RC interaction $H_{\text{int}}^{\text{res}}$ is

$$H_{\text{int}}^{\text{res}} = (a + a^\dagger) \int_0^\infty d\omega \sqrt{2\omega J_{\text{RC}}} x_\omega, \quad (\text{F4})$$

with J_{RC} the spectral density of the residual bath.

Given H_{tot} , for an appropriate choice of J_{RC} (which depends on the original Hamiltonian spectral density and coupling), it has been proven that the reduced dynamics of the spin under H_{tot} are exactly the same as those of the spin under the effective Hamiltonian $H_{\text{tot}}^{\text{RC}}$ [68]. In general, the mapping between the original spectral density, J_ω , and that of the RC Hamiltonian, J_{RC} , is hard to find. However, one particular case where there is a simple closed form for J_{RC} is that of a Lorentzian spectral density J_ω , given by (D1). In such case, the J_{RC} spectral density is exactly Ohmic [66–68], i.e. has the form

$$J_{\text{RC}} = \gamma_{\text{RC}} \omega e^{-\omega/\omega_c}, \quad \omega_c \rightarrow \infty. \quad (\text{F5})$$

Furthermore, the RC effective Hamiltonian parameters (Ω_{RC} , λ_{RC} and γ_{RC}) are given by

$$\Omega_{\text{RC}} = \omega_0, \quad (\text{F6})$$

$$\lambda_{\text{RC}} = \sqrt{Q_{\text{lor}} \omega_0}, \quad (\text{F7})$$

$$\gamma_{\text{RC}} = \frac{\Gamma}{2\pi\omega_0}. \quad (\text{F8})$$

Noticeably, by appropriately choosing A , Γ , and ω_0 , we can have an initial Hamiltonian with arbitrarily strong coupling to the full environment (i.e. arbitrarily strong Q_{lor}), while having arbitrarily small coupling to the residual bath of the RC Hamiltonian (i.e. arbitrarily small γ_{RC}).

As mentioned, it has been shown that the reduced spin dynamics under H_{tot} with spectral density (D1) is exactly the same as the reduced spin dynamics under $H_{\text{tot}}^{\text{RC}}$ with spectral density (F5). In particular, the steady state of the spin will also be the same. Therefore, it is reasonable to expect that the spin MF state obtained with H_{tot} will be the same as the spin MF state for $H_{\text{tot}}^{\text{RC}}$, i.e.

$$\tau_{\text{MF}} = \tilde{Z}_S^{-1} \text{tr}_R [e^{-\beta H_{\text{tot}}}] = \tilde{Z}_S'^{-1} \text{tr}_R [e^{-\beta H_{\text{tot}}^{\text{RC}}}] \quad (\text{F9})$$

We now assume that γ_{RC} is arbitrarily small, so that the MF state is simply going to be given by the Gibbs state of spin+RC, i.e.

$$\tau_{\text{MF}} = \tilde{Z}_S'^{-1} \text{tr}_R [e^{-\beta H_{\text{tot}}^{\text{RC}}}] \approx \tilde{Z}_S''^{-1} \text{tr}_R \left[\exp \left[-\beta (H_S + \Omega_{\text{RC}} a^\dagger a + \lambda_{\text{RC}} S_\theta (a + a^\dagger)) \right] \right]. \quad (\text{F10})$$

It is key here to observe that the condition $\gamma_{\text{RC}} \rightarrow 0$ does not imply any constraint on the coupling strength to the original environment, since we can always choose Γ and ω_0 so that γ_{RC} is arbitrarily small, while also choosing A and ω_0 so that Q_{lor} is arbitrarily large.

Finally, to numerically obtain the MF state, since unfortunately (F10) does not have a general closed form, we numerically evaluate (F10) by diagonalising the full Hamiltonian and then taking the partial trace over the RC. To numerically diagonalise this Hamiltonian we have to choose a cutoff on the number of energy levels of the RC harmonic oscillator. This cutoff was chosen by increasing the number of levels until observing convergence of the numerical results.

Appendix G: Quantum–classical correspondence in the ultrastrong coupling limit

Here, we numerically illustrate the quantum–classical correspondence in the limit of ultrastrong coupling to the environment, which is later formally proven in Supplement J.

Fig. S1 summarises the impact of different corrections when taking the classical Gibbs state (CG) as the reference: purely quantum corrections (QG), classical corrections due to the environment's mean force (CMF), as well as those arising from the combination of quantum and environmental corrections (QMF; obtained using the reaction coordinate method, see Supplement F).

While at weak coupling the classical and quantum predictions are quite different, that difference *decreases* with increasing coupling ζ . In the ultrastrong limit, the two predictions become the same (C(Q)MFUS). This is because the quantum QMFUS partition function $\tilde{Z}_S^{\text{qu}}(\beta, S_0)$ only depends on the product of βS_0 , and thus the quantum to classical transition is trivial, cf. Fig. 3 and the discussion of this transition above.

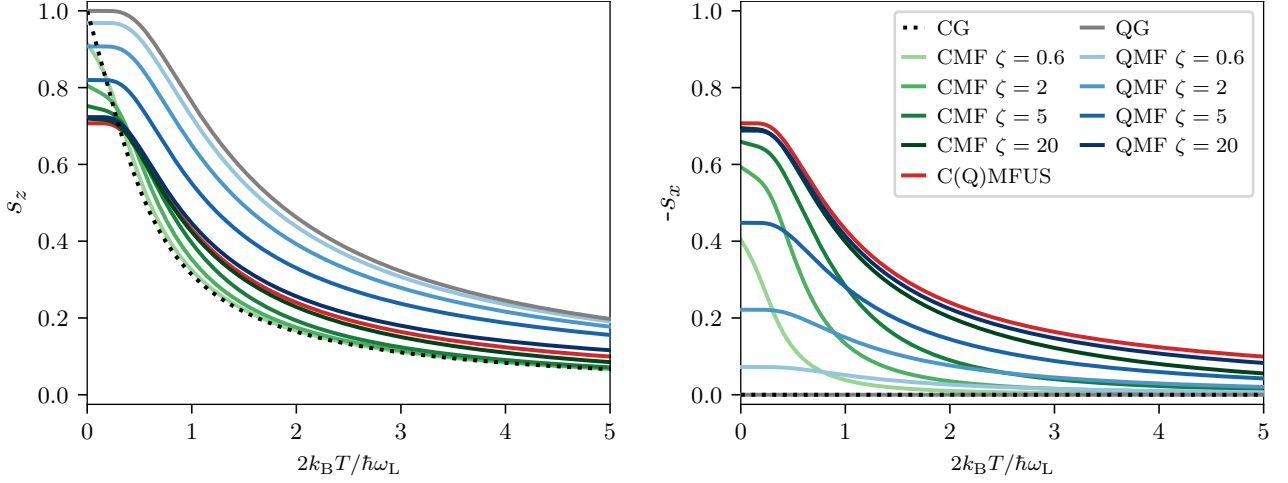


FIG. S1. **Mean force and quantum deviations from classical Gibbs state prediction.** **Left:** The equilibrium s_z component as a function of temperature, computed for the classical Gibbs state (CG, black dotted), is changed very significantly at all non-zero temperatures when the quantum character of the spin is included (quantum Gibbs state (QG), grey dashed). On the other hand, coupling the classical spin to its environment with increasing coupling parameter ζ , also leads to corrections (CMF, solid green, darker for larger ζ), predominantly at low temperatures (e.g. $0 \leq 2k_B T / \hbar\omega_L \leq 2$ for $\zeta = 5$). The combination of quantum and mean force corrections (QMF, solid blue, darker for larger ζ) is calculated using the reaction coordinate method, see Supplement F. Deviations between QMF (blue) and CMF (green) decrease for increasing coupling strength ζ , with both converging to the same curve (C(Q)MFUS, solid red) for $\zeta \rightarrow \infty$. **Right:** Same as on the left but for the environment-induced “coherence” component s_x , which is exactly zero for both the CG and QG states.

Appendix H: Classical version of coupling regimes

Here we report the details of the different coupling regimes for the classical spin. Fig. S2 shows the equivalent plot to Fig. 6 of the main text (which is also plotted again in Fig. S3 for easier comparison) but now for the case of a classical spin. We note that qualitatively speaking there are some similarities. In particular, the classical case also shows a shift at high temperatures of the boundaries that grows linearly with the temperature, i.e. $\zeta \propto T$. However, interestingly, the actual values of the boundaries differ from the quantum case, particularly for the weak coupling, where the difference is of nearly a factor of 10. We show with a red star in Figs. S2 and S3 an example of a coupling strength such that the classical spin is in the intermediate coupling regime while the quantum one is in the weak regime.

Finally, it is worth noting that, while for both the quantum and classical case, the exact value of the boundary depends on the choice of tolerable error (which determines if an approximation is good enough or not) which is somewhat arbitrary, we observed that changing the value only shifts the boundaries in the $T \rightarrow 0$ limit, but does not change the qualitative behaviour shown in Fig. S3 and Fig. S2, nor the asymptotic behaviour or the differences between quantum and classical spin.

Appendix I: Quantum to classical limit in the weak coupling approximation

In this section we check the general validity of the argument given in appendix E about the quantum-to-classical limit by explicitly computing the large spin limit for the weak coupling expressions of the classical and quantum mean force Gibbs states.

Since we are going to perform perturbative expansions in the coupling strength, in what follows we introduce, for book-keeping purposes, an adimensional parameter λ in the interaction, so that H_{int} now reads

$$H_{\text{int}} = \lambda S_\theta \int_0^\infty d\omega C_\omega X_\omega. \quad (11)$$

This will allow us to properly keep track of the order of each term in the expansion. Finally, at the end of the calculations we will take $\lambda = 1$.

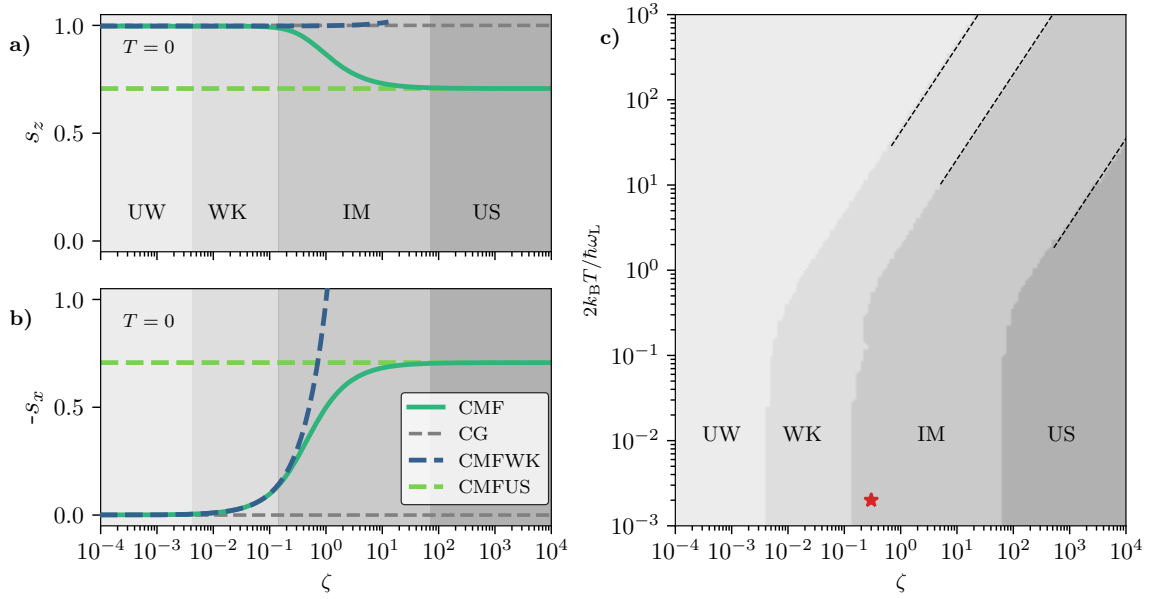


FIG. S2. **Coupling regimes for a classical spin.** a) and b): s_z and $-s_x$ at $T = 0$ for $\theta = \pi/4$ and different coupling strengths as quantified by the parameter ζ (see (10)). We identify four different regimes of coupling strength: (i) Ultraweak coupling (UW), where the spin expectation values are consistent with the Gibbs state (CG, dashed grey) of the bare Hamiltonian H_S ; (ii) Weak coupling (WK), where the expectation values are well approximated by a second order expansion in ζ (CMFWK, dashed blue); (iii) Intermediate coupling (IM), for which higher order corrections cannot be neglected (CMF, solid green); and (iv) Ultrastrong coupling (US), where the asymptotic limit of infinitely strong coupling $\zeta \rightarrow \infty$ is valid (CMFUS, dashed light green). c): Identification of the four different coupling regimes UW, WK, IM, and US as a function of temperature T for $\theta = \pi/4$. With increasing temperature, the boundaries shift towards higher coupling ζ . At large temperatures, all three boundaries follow a linear relation $T \propto \zeta$ (dashed lines). The red star indicates a coupling strength of $\zeta = 0.3$ and temperature $2k_B T / \hbar\omega_L = 0.002$. As can be seen, for the classical spin, this parameter set lies in the intermediate coupling regime (IM), while for the quantum spin this parameter set lies in the weak coupling regime (WK), see Fig. S3.

1. Classical spin: weak coupling

Here, we derive the classical weak coupling expectation values starting from the exact MF found in C. The effective Hamiltonian, with the inclusion of the parameter λ now reads

$$H_{\text{eff}} = -\omega_L S_z - \lambda^2 Q S_\theta^2. \quad (12)$$

For weak coupling, the expressions for \tilde{Z}_S^{cl} , $\langle S_z \rangle$ and $\langle S_x \rangle$ can be approximated by treating the term $\lambda^2 S_\theta^2 Q$ as a perturbation. Therefore, expanding $\exp[-\beta H_{\text{eff}}]$ to lowest order in λ we have

$$e^{-\beta H_{\text{eff}}} = e^{\beta \omega_L S_0 \cos \vartheta} \left[1 + \beta \lambda^2 S_0^2 Q (\cos \theta \cos \vartheta - \sin \theta \sin \vartheta \cos \varphi)^2 \right] + \mathcal{O}(\lambda^4), \quad (13)$$

from which we can determine the weak coupling limit of the classical spin partition function and spin expectation values.

a. Standard Gibbs results for a classical spin

First, here we write the partition function and spin expectation values for a classical spin in the standard Gibbs state for the bare Hamiltonian H_S (i.e. in the limit of vanishing coupling, $\lambda = 0$). These expressions will be useful to later on to write the second order corrections.

For the partition function we have that

$$Z_0^{\text{cl}} = \frac{1}{4\pi} \int_0^{2\pi} d\varphi \int_0^\pi d\vartheta \sin \vartheta \exp[\beta \omega_L S_0 \cos \vartheta] = \frac{\sinh(\beta \omega_L S_0)}{\beta \omega_L S_0}. \quad (14)$$

For S_x we have that is trivially 0 by symmetry, i.e.

$$\langle S_x \rangle_0 = \frac{1}{Z_0^{\text{cl}}} S_0 \int_0^{2\pi} d\varphi \cos \varphi \int_0^\pi d\vartheta \sin^2 \vartheta \exp[\beta \omega_L S_0 \cos \vartheta] = 0. \quad (15)$$

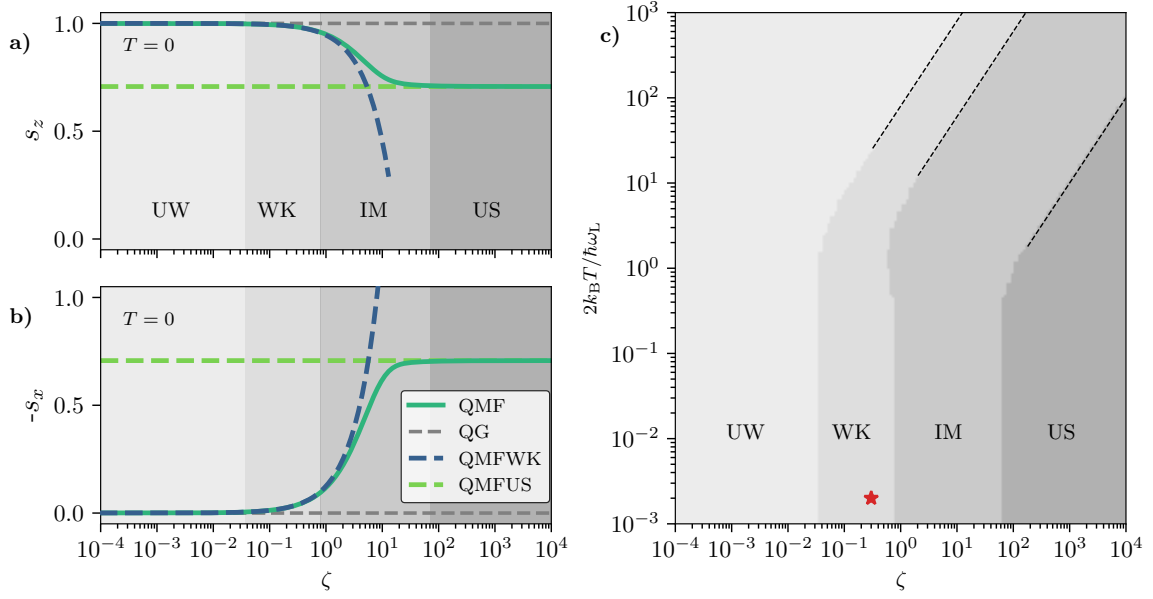


FIG. S3. **Coupling regimes for a quantum spin.** Same plots as shown in Fig. 6 of the main text, but reproduced here for a better direct comparison with the classical case shown in Fig. S2. Of particular significance is that the red star lies within the weak (WK) coupling regimes, contrasting with the classical case Fig. S2.

For the expectation value of S_z its powers (which will be useful later), we have

$$\langle S_z^n \rangle_0 = \frac{2\pi}{Z_0^{\text{cl}}} S_0^n \int_0^\pi d\vartheta \sin \vartheta \cos^n \vartheta \exp[\beta \omega_L S_0 \cos \vartheta]. \quad (16)$$

In particular, we find

$$\langle S_z \rangle_0 = S_0 \coth(\beta \omega_L S_0) - \frac{1}{\beta \omega_L}, \quad (17)$$

$$\langle S_z^2 \rangle_0 = S_0^2 - \frac{2S_0 \coth(\beta \omega_L S_0)}{\beta \omega_L} + \frac{2}{(\beta \omega_L)^2}, \quad (18)$$

$$\langle S_z^3 \rangle_0 = S_0^3 \coth(\beta \omega_L S_0) - \frac{3S_0^2}{\beta \omega_L} + \frac{6S_0 \coth(\beta \omega_L S_0)}{(\beta \omega_L)^2} - \frac{6}{(\beta \omega_L)^3}. \quad (19)$$

b. Classical spin partition function for weak coupling

Expanding the partition function to second order in λ we find that

$$\begin{aligned} \tilde{Z}_S^{\text{cl}} = & \frac{1}{4\pi} \int_0^{2\pi} d\varphi \int_0^\pi d\vartheta \sin \vartheta e^{\beta \omega_L S_0 \cos \vartheta} \\ & + \frac{\beta \lambda^2 S_0^2 Q}{4\pi} \int_0^{2\pi} d\varphi \int_0^\pi d\vartheta \sin \vartheta e^{\beta \omega_L S_0 \cos \vartheta} (\cos \theta \cos \vartheta - \sin \theta \sin \vartheta \cos \varphi)^2 + \mathcal{O}(\lambda^4). \end{aligned} \quad (110)$$

The first term can be recognised as the partition function for the bare system, Z_0 . The φ' integral in the second term is straightforward to perform,

$$\tilde{Z}_S^{\text{cl}} = Z_0^{\text{cl}} + \frac{1}{2} \beta \lambda^2 S_0^2 Q \int_0^\pi d\vartheta \sin \vartheta e^{\beta \omega_L S_0 \cos \vartheta} ((3 \cos^2 \theta - 1) \cos^2 \vartheta + \sin^2 \theta) + \mathcal{O}(\lambda^4). \quad (111)$$

We typically require the inverse of the partition function, which to lowest order in the perturbation is

$$\tilde{Z}_S^{\text{cl}} = (Z_0^{\text{cl}})^{-1} \left[1 - \pi \beta \lambda^2 S_0^2 Q Z_0^{-1} \int_0^\pi d\vartheta \sin \vartheta e^{\beta \omega_L S_0 \cos \vartheta} ((3 \cos^2 \theta - 1) \cos^2 \vartheta + \sin^2 \theta) \right] + \mathcal{O}(\lambda^4). \quad (112)$$

c. Classical $\langle S_z \rangle$ for weak coupling

Now turning to the expectation value $\langle S_z \rangle$, given in Eq. (C9), and carrying out the same lowest order expansion we get

$$\langle s_z \rangle = \frac{\langle S_z \rangle}{S_0} = \frac{1}{\tilde{Z}_S^{\text{cl}}} \left[2\pi \int_0^\pi d\vartheta \sin \vartheta \cos \vartheta e^{\beta \omega_L S_0 \cos \vartheta} + \pi \beta \lambda^2 S_0^2 Q \int_0^\pi d\vartheta \sin \vartheta \cos \vartheta e^{\beta \omega_L S_0 \cos \vartheta} \left((3 \cos^2 \theta - 1) \cos^2 \vartheta + \sin^2 \theta \right) \right] + \mathcal{O}(\lambda^4), \quad (113)$$

which we can write as

$$\langle s_z \rangle = \frac{\langle S_z \rangle}{S_0} = \frac{Z_0^{\text{cl}}}{\tilde{Z}_S^{\text{cl}}} \left[\frac{\langle S_z \rangle_0}{S_0} + \frac{1}{2} \beta \lambda^2 S_0^2 Q \left((3 \cos^2 \theta - 1) \frac{\langle S_z^3 \rangle_0}{S_0^3} + \sin^2 \theta \frac{\langle S_z \rangle_0}{S_0} \right) \right] + \mathcal{O}(\lambda^4). \quad (114)$$

Making use of the lowest order expansion for $1/\tilde{Z}_S^{\text{cl}}$ we get

$$\langle S_z \rangle = \langle S_z \rangle_0 + \frac{1}{2} \beta \lambda^2 Q \left[(3 \cos^2 \theta - 1) (\langle S_z^3 \rangle_0 - \langle S_z \rangle_0 \langle S_z^2 \rangle_0) \right] + \mathcal{O}(\lambda^4). \quad (115)$$

Finally, using the zeroth order expressions for $\langle S_z \rangle_0$, $\langle S_z^2 \rangle_0$ and $\langle S_z^3 \rangle_0$ from (17) we get the result

$$\langle S_z \rangle = S_0 \coth(\beta \omega_L S_0) - \frac{1}{\beta \omega_L} + \frac{\lambda^2 S_0^2 Q}{\omega_L} (3 \cos^2 \theta - 1) \left(\text{cosech}^2(\beta \omega_L S_0) + \frac{\coth(\beta \omega_L S_0)}{\beta \omega_L S_0} - \frac{2}{(\beta \omega_L S_0)^2} \right) + \mathcal{O}(\lambda^4), \quad (116)$$

which, when written in terms of the scaled temperature $\beta' = \beta S_0$ becomes

$$\langle s_z \rangle = \coth(\beta' \omega_L) - \frac{1}{\beta' \omega_L} + \frac{\lambda^2 S_0 Q}{2 \omega_L} (1 + 3 \cos 2\theta) \left(\text{cosech}^2(\beta' \omega_L) + \frac{\coth(\beta' \omega_L)}{\beta' \omega_L} - \frac{2}{(\beta' \omega_L)^2} \right) + \mathcal{O}(\lambda^4). \quad (117)$$

This result will be compared later to the quantum weak coupling result obtained in the large spin (classical) limit.

d. Classical $\langle S_x \rangle$ for weak coupling

A similar calculation can be followed for $\langle S_x \rangle$, the main difference being in the handling of the φ' integral. Thus, we find

$$\langle S_x \rangle = -\frac{1}{2} \sin 2\theta \beta \lambda^2 Q (\langle S_z \rangle_0 S_0^2 - \langle S_z^3 \rangle_0) + \mathcal{O}(\lambda^4), \quad (118)$$

where we have used that $Z_0/\tilde{Z}_S^{\text{cl}} = 1$ to lowest order.

Using the zeroth order expressions for $\langle S_z \rangle_0$ and $\langle S_z^3 \rangle_0$ from (17) we get the result in terms of the scaled temperature $\beta' = \beta S_0$

$$\langle s_x \rangle = -\frac{\sin 2\theta \lambda^2 S_0 Q}{\omega_L} \left(1 - \frac{3 \coth(\beta' \omega_L)}{\beta' \omega_L} + \frac{3}{(\beta' \omega_L)^2} \right) + \mathcal{O}(\lambda^4). \quad (119)$$

This result will be compared later to the quantum weak coupling result obtained in the large spin (classical) limit.

2. Quantum spin: weak coupling

In general, the quantum mean force Gibbs state is given by

$$\tau_{\text{MF}} = \frac{\text{tr}_R^{\text{qu}} [e^{-\beta H_{\text{tot}}}] }{Z_{\text{tot}}^{\text{qu}}}, \quad (120)$$

with H_{tot} given by Eq. (3) of the main text. Unfortunately, determining the form of τ_{MF} and the various expectation values for the spin components is unfeasible in the general case, but limiting forms are available. Here we derive the spin expectation values in the weak coupling limit, and then later on take the large spin limit to explicitly verify the quantum-to-classical transition.

a. *Standard Gibbs results for a quantum spin*

Here, we present the results of the standard Gibbs state for the quantum spin (i.e. in the limit of vanishing coupling, $\lambda = 0$). The Gibbs state for the system's bare Hamiltonian is

$$\tau_S = \frac{e^{\beta\omega_L S_z}}{Z_S^{\text{qu}}}, \quad Z_S^{\text{qu}} = \text{tr} [e^{\beta\omega_L S_z}]. \quad (121)$$

We also have that $[\tau_S, S_z] = 0$. The trace is readily evaluated, yielding the partition function

$$Z_0^{\text{qu}} = \frac{\sinh \beta\omega_L (S_0 + \frac{\hbar}{2})}{\sinh \frac{\hbar}{2} \beta\omega_L}, \quad (122)$$

from which we can derive the expectation values of S_z , S_z^2 and S_z^3 ,

$$\langle S_z^n \rangle_0 = \frac{1}{Z_0^{\text{qu}}} \frac{d^n}{d(\beta\omega_L)^n} Z_0^{\text{qu}}, \quad (123)$$

where $\langle \dots \rangle_0 = \text{tr} [\tau_S \dots]$. We find,

$$\begin{aligned} \langle S_z \rangle_0 &= (S_0 + \frac{\hbar}{2}) \coth(\beta\omega_L (S_0 + \frac{\hbar}{2})) - \frac{\hbar}{2} \coth(\frac{\hbar}{2} \beta\omega_L) \\ \langle S_z^2 \rangle_0 &= (S_0 + \frac{\hbar}{2})^2 - \hbar(S_0 + \frac{\hbar}{2}) \coth(\frac{\hbar}{2} \beta\omega_L) \coth(\beta\omega_L (S_0 + \frac{\hbar}{2})) + \frac{\hbar^2}{4} (2 \coth^2(\frac{\hbar}{2} \beta\omega_L) - 1) \\ \langle S_z^3 \rangle_0 &= (S_0 + \frac{\hbar}{2})^3 \coth(\beta\omega_L (S_0 + \frac{\hbar}{2})) - \frac{3\hbar}{2} (S_0 + \frac{\hbar}{2})^2 \coth(\frac{\hbar}{2} \beta\omega_L) \\ &\quad + \frac{3\hbar^2}{4} (S_0 + \frac{\hbar}{2}) \coth(\beta\omega_L (S_0 + \frac{\hbar}{2})) (2 \coth^2(\frac{\hbar}{2} \beta\omega_L) - 1) - \frac{3\hbar^3}{4} \coth^3(\frac{\hbar}{2} \beta\omega_L) + \frac{5\hbar^3}{8} \coth(\frac{\hbar}{2} \beta\omega_L). \end{aligned} \quad (124)$$

b. *General form of weak coupling density operator*

For the Hamiltonian without counter term, and an interaction of the form $H_{\text{int}} = \lambda X B$, the general expression for the *unnormalised* mean force state to second order in the interaction is given by [33]

$$\tilde{\rho}^{(2)} = \tau_S + \lambda^2 \sum_n ([X_n^\dagger, \tau_S X_n] A'_\beta(\omega_n) + \beta \tau_S X_n X_n^\dagger A_\beta(\omega_n)) + \lambda^2 \sum_{m \neq n} \omega_{mn}^{-1} ([X_m, X_n^\dagger \tau_S] + [\tau_S X_n, X_m^\dagger]) A_\beta(\omega_n), \quad (125)$$

where the system operator X is expanded in terms of the energy eigenoperators X_n

$$X = \sum_n X_n, \quad (126)$$

with $[H_S, X_n] = \omega_n X_n$, and ω_n are Bohr frequencies for the system. We have $X_n^\dagger = X_{-n}$ and $\omega_n = -\omega_{-n}$. The quantities $A_\beta(\omega_n)$ are determined by the correlation properties of the reservoir operator B and are given by

$$A_\beta(\omega_n) = \int_0^\infty d\omega J_\omega \left(\frac{n_\beta(\omega) + 1}{\omega - \omega_n} - \frac{n_\beta(\omega)}{\omega + \omega_n} \right), \quad (127)$$

$$A'_\beta(\omega_n) = \int_0^\infty d\omega \frac{J_\omega}{\hbar} \left(\frac{n_\beta(\omega) + 1}{(\omega - \omega_n)^2} + \frac{n_\beta(\omega)}{(\omega + \omega_n)^2} \right). \quad (128)$$

We can separate out the particular case of $\omega_n = 0$, for which we find

$$A_\beta(0) = \int_0^\infty d\omega \frac{J_\omega}{\omega} = Q. \quad (129)$$

It turns out that we will require various symmetric and antisymmetric combinations of $A_\beta(\omega_n)$ and $A'_\beta(\omega_n)$. [Note that in the following (and in the initial definition of the quantity $A'_\beta(\omega_n)$), the dash indicates a derivative wrt to the argument ω_n . Thus the quantity $A'_\beta(-\omega_n)$ is a derivative wrt $-\omega_n$, i.e., $A'_\beta(-\omega_n) = -dA_\beta(-\omega_n)/d\omega_n$, whereas, as usual, $A'_\beta(\omega_n) = dA_\beta(\omega_n)/d\omega_n$ etc.] Therefore, we define

$$\Sigma(\omega_n) = A_\beta(\omega_n) + A_\beta(-\omega_n) = 2 \int_0^\infty d\omega J_\omega \frac{\omega}{\omega^2 - \omega_n^2} \quad (130)$$

$$\Delta_\beta(\omega_n) = A_\beta(\omega_n) - A_\beta(-\omega_n) = 2\omega_n \int_0^\infty d\omega J_\omega \frac{1}{\omega^2 - \omega_n^2} \coth(\frac{1}{2}\beta\hbar\omega) \quad (131)$$

$$\Delta'_\beta(\omega_n) = A'_\beta(\omega_n) + A'_\beta(-\omega_n) = 2 \int_0^\infty d\omega \frac{J_\omega}{\hbar} \frac{(\omega^2 + \omega_n^2)}{(\omega^2 - \omega_n^2)^2} \coth(\frac{1}{2}\beta\hbar\omega) \quad (132)$$

$$\Sigma'(\omega_n) = A'_\beta(\omega_n) - A'_\beta(-\omega_n) = 4\omega_n \int_0^\infty d\omega \frac{J_\omega}{\hbar} \frac{\omega}{(\omega^2 - \omega_n^2)^2}. \quad (133)$$

c. *Normalising the second order MF*

From (125) we get the second order partition function

$$\tilde{Z}_S^{(2)} = \text{tr}[\tilde{\rho}^{(2)}] = 1 + \beta\lambda^2 \sum_n \text{tr} [\tau_S X_n X_n^\dagger] A_\beta(\omega_n). \quad (134)$$

This can be used directly to evaluate the second order expectation value $\langle S_z \rangle^{(2)}$, but instead we will proceed to derive the second order MF. This normalised state can be arrived at in two ways. First we can write

$$\tau_{\text{MF}}^{(2)} = \frac{\tilde{\rho}^{(2)}}{\tilde{Z}_S^{(2)}}, \quad (135)$$

and then, on the basis that the second order correction in (134) is $\ll 1$, we can make the binomial approximation

$$\frac{1}{\tilde{Z}_S^{(2)}} = 1 - \beta\lambda^2 \sum_n \text{tr} [\tau_S X_n X_n^\dagger] A_\beta(\omega_n), \quad (136)$$

in which case the normalised state is, correct to second order

$$\begin{aligned} \tau_{\text{MF}}^{(2)} &= \tau_S + \lambda^2 \sum_n [[X_n^\dagger, \tau_S X_n] A'_\beta(\omega_n) + \beta\tau_S (X_n X_n^\dagger - \text{tr} [\tau_S X_n X_n^\dagger]) A_\beta(\omega_n)] \\ &\quad + \lambda^2 \sum_{m \neq n} \omega_{mn}^{-1} ([X_m, X_n^\dagger \tau_S] + [\tau_S X_n, X_m^\dagger]) A_\beta(\omega_n). \end{aligned} \quad (137)$$

The issue with this approach is that it assumes the validity of the binomial approximation, which requires the second order correction to $\tilde{Z}_S^{(2)}$ to be $\ll 1$. However, this term grows linearly with β , so that at a sufficiently low temperature this second order correction will exceed unity by an arbitrary amount, and the binomial approximation cannot be justified.

An alternate approach is to deal directly with the exact density operator

$$\tau_{\text{MF}}(\lambda) = \frac{\tilde{\rho}(\lambda)}{\tilde{Z}_S^{\text{qu}}(\lambda)}, \quad (138)$$

where the dependence on λ is made explicit, and write

$$\tau_{\text{MF}}(\lambda) = \tau_{\text{MF}}(0) + \frac{1}{2}\lambda^2 \frac{d^2 \tau_{\text{MF}}}{d\lambda^2}(0) + \mathcal{O}(\lambda^4), \quad (139)$$

where $\tau_{\text{MF}}(0) = \tau_S$ is the Gibbs state of the system in the limit of vanishingly small system-reservoir coupling, and it has been recognised that odd order contributions will vanish.

From this we also find

$$\tilde{Z}_S^{\text{qu}}(\lambda) = 1 + \frac{1}{2}\lambda^2 \frac{d^2 \tilde{Z}_S^{\text{qu}}}{d\lambda^2}(0) + \mathcal{O}(\lambda^4). \quad (140)$$

If we now do a Taylor series expansion of $\tau_{\text{MF}}(\lambda)$ we find, using $\tilde{Z}_S^{\text{qu}}(0) = 1$,

$$\tau_{\text{MF}}(\lambda) = \tau_S + \frac{1}{2}\lambda^2 \left(\frac{d^2 \tilde{\rho}}{d\lambda^2}(0) - \frac{d^2 \tilde{Z}_S^{\text{qu}}}{d\lambda^2}(0) \tau_S \right) + \mathcal{O}(\lambda^4) \quad (141)$$

$$= \tau_S + \lambda^2 \sum_n [[X_n^\dagger, \tau_S X_n] A'_\beta(\omega_n) + \beta\tau_S (X_n X_n^\dagger - \text{tr} [\tau_S X_n X_n^\dagger]) A_\beta(\omega_n)] \quad (142)$$

$$+ \sum_{m \neq n} \omega_{mn}^{-1} ([X_m, X_n^\dagger \tau_S] + [\tau_S X_n, X_m^\dagger]) A_\beta(\omega_n) + \mathcal{O}(\lambda^4). \quad (143)$$

So we regain (137), but without having to consider any restrictions on β . In contrast the binomial expansion based derivation seems to imply that irrespective of the choice of coupling strength, there will always be a temperature below which the binomial approximation will fail and (137) can lead to incorrect results below this temperature. But this argument cannot be sustained as the validity of the second order expansion is not constrained by any lower temperature limit implied by the binomial expansion as it can be obtained without making this approximation.

What we now have is the necessary requirement that (for some definition of the norm $\|\dots\|$ of the operators involved)

$$\frac{1}{2}\lambda^2 \left\| \left(\frac{d^2 \tau_{\text{MF}}}{d\lambda^2}(0) - \tau_{\text{S}} \frac{d^2 \tilde{Z}_{\text{S}}^{\text{qu}}}{d\lambda^2}(0) \right) \right\| \ll \|\tau_{\text{S}}\|, \quad (144)$$

for the second order result (137) to be valid. This of course is not a sufficient condition as the higher order terms, $\mathcal{O}(\lambda^4)$, are not guaranteed to be negligible.

The concern is the low temperature limit $\beta \rightarrow \infty$, where the term linear in β seems to imply linear divergence so the condition (144) cannot be met. However, it can be shown that in this limit the second order correction term in (137) actually vanishes [33]. It also does so for $\beta \rightarrow 0$, the high temperature limit, so there might be an intermediate temperature for which the condition (144) is not satisfied, this then requiring a weaker interaction coupling strength.

The conclusion then is that for sufficiently weak coupling, the result (137) will hold true for all temperatures.

d. Detailed derivation of the normalised second order MF

To evaluate the second order expression for the normalised density operator given by (137) we need to expand $X = S_\theta$ in terms of the energy eigenoperators X_n ,

$$X = S_z \cos \theta - S_x \sin \theta = -\frac{1}{2} \sin \theta S_- + \cos \theta S_z - \frac{1}{2} \sin \theta S_+, \quad (145)$$

so we can identify, from $X = X_{-1} + X_0 + X_{+1}$,

$$X_{-1} = -\frac{1}{2} \sin \theta S_-, \quad X_0 = \cos \theta S_z, \quad X_{+1} = -\frac{1}{2} \sin \theta S_+. \quad (146)$$

To determine the corresponding eigenfrequencies, we use $[H_{\text{S}}, X_n] = \omega_n X_n$ and find that

$$[H_{\text{S}}, X_{-1}] = [-\omega_{\text{L}} S_z, -\frac{1}{2} \sin \theta S_-] = \omega_{\text{L}} X_{-1}, \quad (147)$$

and hence $\omega_{-1} = \omega_{\text{L}}$. It follows that $\omega_{+1} = -\omega_{\text{L}}$, and by inspection, $\omega_0 = 0$.

We then have a number of sums to evaluate, and doing so yields

$$\begin{aligned} \tau_{\text{MF}}^{(2)} = & \tau_{\text{S}} + \frac{1}{4}\lambda^2 \sin^2 \theta ([S_+, \tau_{\text{S}} S_-] A'_\beta(\omega_{\text{L}}) + \beta \tau_{\text{S}} (S_- S_+ - \text{tr} [\tau_{\text{S}} S_- S_+]) A_\beta(\omega_{\text{L}})) \\ & + \lambda^2 \cos^2 \theta \beta \tau_{\text{S}} (S_z^2 - \text{tr} [\tau_{\text{S}} S_z^2]) Q \\ & + \frac{1}{4}\lambda^2 \sin^2 \theta ([S_-, \tau_{\text{S}} S_+] A'_\beta(-\omega_{\text{L}}) + \beta \tau_{\text{S}} (S_+ S_- - \text{tr} [\tau_{\text{S}} S_+ S_-]) A_\beta(-\omega_{\text{L}})) \\ & + (2\omega_{\text{L}})^{-1} \lambda^2 \sin \theta \cos \theta ([S_z, S_+ \tau_{\text{S}}] + [\tau_{\text{S}} S_-, S_z]) A_\beta(\omega_{\text{L}}) \\ & - (8\omega_{\text{L}})^{-1} \lambda^2 \sin^2 \theta ([S_+, S_+ \tau_{\text{S}}] + [\tau_{\text{S}} S_-, S_-]) A_\beta(\omega_{\text{L}}) \\ & - (2\omega_{\text{L}})^{-1} \lambda^2 \sin \theta \cos \theta ([S_-, S_z \tau_{\text{S}}] + [\tau_{\text{S}} S_z, S_+]) Q \\ & + (2\omega_{\text{L}})^{-1} \lambda^2 \sin \theta \cos \theta ([S_+, S_z \tau_{\text{S}}] + [\tau_{\text{S}} S_z, S_-]) Q \\ & + (8\omega_{\text{L}})^{-1} \lambda^2 \sin^2 \theta ([S_-, S_- \tau_{\text{S}}] + [\tau_{\text{S}} S_+, S_+]) A_\beta(-\omega_{\text{L}}) \\ & - (2\omega_{\text{L}})^{-1} \lambda^2 \sin \theta \cos \theta ([S_z, S_- \tau_{\text{S}}] + [\tau_{\text{S}} S_+, S_z]) A_\beta(-\omega_{\text{L}}). \end{aligned} \quad (148)$$

We can then calculate the expectation values of S_z and S_x from this result. The calculation of these quantities is made 'easier' by the fact that τ_{S} is diagonal in the S_z basis, and that $\langle S_y \rangle = 0$.

e. Quantum $\langle S_z \rangle$ for weak coupling

The S_z expectation value will be given by

$$\begin{aligned} \langle S_z \rangle^{(2)} = & \text{tr} [S_z \tau_{\text{S}}] + \frac{1}{4}\lambda^2 \sin^2 \theta (\text{tr} [S_z [S_+, \tau_{\text{S}} S_-]] A'_\beta(\omega_{\text{L}}) + \beta (\text{tr} [S_z \tau_{\text{S}} S_- S_+] - \text{tr} [\tau_{\text{S}} S_z] \text{tr} [\tau_{\text{S}} S_- S_+]) A_\beta(\omega_{\text{L}})) \\ & + \lambda^2 \cos^2 \theta \beta (\text{tr} [\tau_{\text{S}} S_z^3] - \text{tr} [\tau_{\text{S}} S_z] \text{tr} [\tau_{\text{S}} S_z^2]) Q \\ & + \frac{1}{4}\lambda^2 \sin^2 \theta (\text{tr} [S_z [S_-, \tau_{\text{S}} S_+]] A'_\beta(-\omega_{\text{L}}) + \beta (\text{tr} [S_z \tau_{\text{S}} S_+ S_-] - \text{tr} [\tau_{\text{S}} S_z] \text{tr} [\tau_{\text{S}} S_+ S_-]) A_\beta(-\omega_{\text{L}})). \end{aligned} \quad (149)$$

We find that, on setting $\text{tr}[\tau_S \dots] = \langle \dots \rangle_0$,

$$\begin{aligned}\text{tr}[S_z \tau_S S_- S_+] &= S_0(S_0 + \hbar) \langle S_z \rangle_0 - \langle S_z^3 \rangle_0 - \hbar \langle S_z^2 \rangle_0 \\ \text{tr}[S_z [S_+, \tau_S S_-]] &= \hbar S_0(S_0 + \hbar) - \hbar \langle S_z^2 \rangle_0 - \hbar^2 \langle S_z \rangle_0 \\ \text{tr}[S_z \tau_S S_+ S_-] &= S_0(S_0 + \hbar) \langle S_z \rangle_0 - \langle S_z^3 \rangle_0 + \hbar \langle S_z^2 \rangle_0 \\ \text{tr}[S_z [S_-, \tau_S S_+]] &= -\hbar S_0(S_0 + \hbar) + \hbar \langle S_z^2 \rangle_0 - \hbar^2 \langle S_z \rangle_0.\end{aligned}\quad (150)$$

Thus, we get

$$\begin{aligned}\langle S_z \rangle^{(2)} &= \langle S_z \rangle_0 + \frac{1}{4} \hbar \lambda^2 \sin^2 \theta ((S_0(S_0 + \hbar) - \langle S_z^2 \rangle_0) \Sigma'(\omega_L) - \langle S_z \rangle_0 \hbar \Delta'_\beta(\omega_L)) \\ &\quad - \beta \lambda^2 \left[\frac{1}{4} \sin^2 \theta ((\langle S_z^2 \rangle_0 - \langle S_z \rangle_0^2) \hbar \Delta_\beta(\omega_L) + (\langle S_z^3 \rangle_0 - \langle S_z \rangle_0 \langle S_z^2 \rangle_0) \Sigma(\omega_L)) - \cos^2 \theta (\langle S_z^3 \rangle_0 - \langle S_z \rangle_0 \langle S_z^2 \rangle_0) Q \right].\end{aligned}\quad (151)$$

f. Quantum $\langle S_x \rangle$ for weak coupling

This is most easily calculated by evaluating $\langle S_+ \rangle$, and using its properties as a raising operator to simplify the exclusion of terms that can be readily seen to vanish, and of course relying on the fact that $\langle S_y \rangle = 0$. The latter actually emerges by calculating $\langle S_+ \rangle$, and as this turns out to be a real quantity, the contribution due to $i \langle S_y \rangle$ from evaluating $\langle S_+ \rangle$ must be zero.

A simple calculation then gives

$$\langle S_x \rangle^{(2)} = \lambda^2 \frac{\sin \theta \cos \theta}{2\omega_L} [\langle S_- S_+ \rangle_0 A_\beta(\omega_L) + \langle S_+ S_- \rangle_0 A_\beta(-\omega_L) - 4 \langle S_z^2 \rangle_0 Q]. \quad (152)$$

Substituting for $S_- S_+$ and $S_+ S_-$ we get

$$\langle S_x \rangle^{(2)} = \lambda^2 \frac{\sin 2\theta}{4\omega_L} [(S_0(S_0 + \hbar) - \langle S_z^2 \rangle_0) \Sigma(\omega_L) - \hbar \langle S_z \rangle_0 \Delta_\beta(\omega_L) - 4 \langle S_z^2 \rangle_0 Q]. \quad (153)$$

3. Quantum to classical limit for weak coupling

In what follows we explicitly verify the quantum to classical transition in the large spin limit presented in E, using the quantum and classical weak coupling expressions found in the previous sections.

First, (151), we have $\langle S_z \rangle$, regrouped to read

$$\begin{aligned}\langle S_z \rangle &= \langle S_z \rangle_0 + \frac{1}{4} \lambda^2 \sin^2 \theta \times \\ &\quad [(S_0(S_0 + \hbar) - \langle S_z^2 \rangle_0) \hbar \Sigma' - \langle S_z \rangle_0 \hbar^2 \Delta'_\beta - \beta ((\langle S_z^2 \rangle_0 - \langle S_z \rangle_0^2) \hbar \Delta_\beta + (\langle S_z^3 \rangle_0 - \langle S_z \rangle_0 \langle S_z^2 \rangle_0) (\Sigma - 2Q))] \\ &\quad + \frac{1}{4} \beta \lambda^2 (1 + 3 \cos 2\theta) Q (\langle S_z^3 \rangle_0 - \langle S_z \rangle_0 \langle S_z^2 \rangle_0).\end{aligned}\quad (154)$$

Introducing the scaled temperature $\beta' = \beta S_0$ and the scaled spin $s_z = S_z/S_0$ and taking the limit $S_0 \rightarrow \infty$ with β' held constant gives

$$\begin{aligned}\langle s_z \rangle &= \langle s_z \rangle_0 + \frac{1}{4} \lambda^2 \sin^2 \theta \times \\ &\quad [(1 - \langle s_z^2 \rangle_0) \hbar (S_0 \Sigma') - \langle s_z \rangle_0 \hbar^2 \Delta'_\beta - \beta' ((\langle s_z^2 \rangle_0 - \langle s_z \rangle_0^2) \hbar \Delta_\beta + (\langle s_z^3 \rangle_0 - \langle s_z \rangle_0 \langle s_z^2 \rangle_0) ((S_0 \Sigma) - 2S_0 Q))] \\ &\quad + \frac{1}{4} \beta' \lambda^2 (1 + 3 \cos 2\theta) (S_0 Q) (\langle s_z^3 \rangle_0 - \langle s_z \rangle_0 \langle s_z^2 \rangle_0).\end{aligned}\quad (155)$$

with (and noting that $S_0 J_\omega$ is independent of S_0)

$$S_0 \Sigma \rightarrow \int_0^\infty (S_0 J_\omega) \frac{2\omega}{\omega^2 - \omega_L^2} d\omega \quad (156)$$

$$\Delta_\beta \rightarrow \int_0^\infty \frac{(S_0 J_\omega)}{\hbar} \frac{4\omega_L}{\omega^2 - \omega_L^2} \cdot \frac{1}{\beta' \omega} d\omega \quad (157)$$

$$\Delta'_\beta \rightarrow \int_0^\infty \frac{(S_0 J_\omega)}{\hbar^2} \frac{4(\omega^2 + \omega_L^2)}{(\omega^2 - \omega_L^2)^2} \cdot \frac{1}{\beta' \omega} d\omega \quad (158)$$

$$S_0 \Sigma' \rightarrow \int_0^\infty \frac{(S_0 J_\omega)}{\hbar} \frac{4\omega_L \omega}{(\omega^2 - \omega_L^2)^2} d\omega \quad (159)$$

$$S_0 Q \rightarrow \int_0^\infty (S_0 J_\omega) \frac{1}{\omega} d\omega. \quad (160)$$

Making use of the $S_0 \rightarrow \infty$ limit of $\langle s_z^n \rangle_0$, $n = 1, 2, 3$ with β' held constant, given from (I24) by the classical forms (I7):

$$\begin{aligned}\langle s_z \rangle_0 &= \coth(\beta' \omega_L) - \frac{1}{\beta' \omega_L} \\ \langle s_z^2 \rangle_0 &= 1 - \frac{2 \coth(\beta' \omega_L)}{\beta' \omega_L} + \frac{2}{(\beta' \omega_L)^2} \\ \langle s_z^3 \rangle_0 &= \coth(\beta' \omega_L) - \frac{3}{\beta' \omega_L} + \frac{6 \coth(\beta' \omega_L)}{(\beta' \omega_L)^2} - \frac{6}{(\beta' \omega_L)^3},\end{aligned}\quad (I61)$$

and the above limiting forms for the integrals, we find that the factor multiplying $\sin^2 \theta$ vanishes and we are left with

$$\langle s_z \rangle = \langle s_z \rangle_0 + \frac{1}{4} \beta' \lambda^2 S_0 Q (1 + 3 \cos 2\theta) (\langle s_z^3 \rangle_0 - \langle s_z \rangle_0 \langle s_z^2 \rangle_0) \quad (I62)$$

which on substituting for the $\langle s_z^n \rangle_0$ yields a result formally identical to the fully classical result, (I17). In a similar way we can check the large spin limit for $\langle S_x \rangle$, and we regain the classical result, (I19).

Appendix J: Ultrastrong coupling limit

In this section we examine ultrastrong coupling limit of the quantum and classical MF.

1. Classical ultrastrong coupling limit

The general expression for this partition function is, from (C6)

$$Z_S^{\text{cl}} = Z_0^{\text{cl}} \int_0^{2\pi} d\varphi' \int_0^\pi d\theta' \sin \theta' \exp \left[\beta \omega_L S_0 \cos \theta' + \frac{1}{2} \beta \lambda^2 S_0^2 Q (\sin \theta \sin \theta' \cos \varphi' - \cos \theta \cos \theta')^2 \right]. \quad (J1)$$

The ultrastrong limit is then the limit in which λ is made very large, in principle taken to infinity. The above expression for the partition function can be written as

$$Z_S^{\text{cl}} = Z_0^{\text{cl}} \int_0^\pi d\theta' \sin \theta' e^{\beta \omega_L S_0 \cos \theta'} F(\lambda, \theta, \theta'). \quad (J2)$$

where

$$F(\lambda, \theta, \theta') = \int_0^{2\pi} d\varphi' \exp \left[\frac{1}{2} \beta \lambda^2 S_0^2 Q (\sin \theta \sin \theta' \cos \varphi' - \cos \theta \cos \theta')^2 \right]. \quad (J3)$$

a. The φ' integral

Defining $a = \frac{1}{2} \beta Q S_0^2$ and expanding the exponent gives

$$\begin{aligned}F(\lambda, \theta, \theta') &= e^{a \lambda^2 \cos^2 \theta \cos^2 \theta'} \int_0^{2\pi} d\varphi' \exp \left[a \lambda^2 (\sin^2 \theta \sin^2 \theta' \cos^2 \varphi' - \frac{1}{2} \sin 2\theta \sin 2\theta' \cos \varphi') \right] \\ &= e^{a \lambda^2 \cos^2 \theta \cos^2 \theta'} \int_0^{2\pi} d\varphi' \exp \left[a \lambda^2 \sin \theta \sin \theta' (\sin \theta \sin \theta' \cos^2 \varphi' - 2 \cos \theta \cos \theta' \cos \varphi') \right].\end{aligned}\quad (J4)$$

For $0 < \theta', \theta \leq 2\pi$, we have $\sin \theta' \sin \theta \geq 0$, but $\cos \theta' \cos \theta$ could be either positive or negative. So we will break up this integral as

$$\begin{aligned}&F(\lambda, \theta, \theta') e^{-a \lambda^2 \cos^2 \theta \cos^2 \theta'} \\ &= \int_0^{2\pi} d\varphi' \exp \left[a \lambda^2 (\sin^2 \theta \sin^2 \theta' (1 - \sin^2 \varphi') - \frac{1}{2} \sin 2\theta \sin 2\theta' (2 \cos^2(\varphi'/2) - 1)) \right] H(\cos \theta' \cos \theta) \\ &\quad + \int_0^{2\pi} d\varphi' \exp \left[a \lambda^2 (\sin^2 \theta \sin^2 \theta' (1 - \sin^2 \varphi') - \frac{1}{2} \sin 2\theta \sin 2\theta' (1 - 2 \sin^2(\varphi'/2))) \right] H(-\cos \theta' \cos \theta),\end{aligned}\quad (J5)$$

where $H(x)$ is the Heaviside step function. This can then be written

$$\begin{aligned}
F(\lambda, \theta, \theta') & e^{-a\lambda^2 \cos^2 \theta \cos^2 \theta'} e^{-a\lambda^2 \sin^2 \theta' \sin^2 \theta} \\
&= e^{\frac{1}{2}a\lambda^2 \sin 2\theta' \sin 2\theta} \int_0^{2\pi} d\varphi' \exp \left[-a\lambda^2 \left(\sin^2 \theta \sin^2 \theta' \sin^2 \varphi' + \sin 2\theta \sin 2\theta' \cos^2(\varphi'/2) \right) \right] H(\cos \theta' \cos \theta) \\
&\quad + e^{-\frac{1}{2}a\lambda^2 \sin 2\theta' \sin 2\theta} \int_0^{2\pi} d\varphi' \exp \left[-a\lambda^2 \left(\sin^2 \theta \sin^2 \theta' \sin^2 \varphi' - \sin 2\theta \sin 2\theta' \sin^2(\varphi'/2) \right) \right] H(-\cos \theta' \cos \theta) \\
&= e^{\frac{1}{2}a\lambda^2 \sin 2\theta' \sin 2\theta} \int_0^{2\pi} d\varphi' \exp \left[-4a\lambda^2 \sin \theta \sin \theta' \cos^2(\varphi'/2) \left(\sin \theta \sin \theta' \sin^2(\varphi'/2) + \cos \theta \cos \theta' \right) \right] H(\cos \theta' \cos \theta) \\
&\quad + e^{-\frac{1}{2}a\lambda^2 \sin 2\theta' \sin 2\theta} \int_0^{2\pi} d\varphi' \exp \left[-4a\lambda^2 \sin \theta \sin \theta' \sin^2(\varphi'/2) \left(\sin \theta \sin \theta' \cos^2(\varphi'/2) - \cos \theta \cos \theta' \right) \right] H(-\cos \theta' \cos \theta),
\end{aligned} \tag{J6}$$

where the exponents in the integrands are now all negative over the range of integration.

This can be made slightly simpler:

$$\begin{aligned}
F(\lambda, \theta, \theta') &= e^{a\lambda^2 \cos^2(\theta' - \theta)} \int_0^{2\pi} d\varphi' \exp \left[-4a\lambda^2 \sin \theta \sin \theta' \cos^2(\varphi'/2) \left(\sin \theta \sin \theta' \sin^2(\varphi'/2) + \cos \theta \cos \theta' \right) \right] H(\cos \theta' \cos \theta) \\
&\quad + e^{a\lambda^2 \cos^2(\theta' + \theta)} \int_0^{2\pi} d\varphi' \exp \left[-4a\lambda^2 \sin \theta \sin \theta' \sin^2(\varphi'/2) \left(\sin \theta \sin \theta' \cos^2(\varphi'/2) - \cos \theta \cos \theta' \right) \right] H(-\cos \theta' \cos \theta).
\end{aligned} \tag{J7}$$

The exponent of the integrand for the first integral where $\cos \theta' \cos \theta > 0$ will vanish at $\varphi' = \pi$, while for the second integral, where $\cos \theta' \cos \theta < 0$, the exponent of the integrand will vanish at $\varphi' = 0, 2\pi$. At these points the integrands will have local maxima which will become increasingly sharp as λ is increased. The second integral is slightly awkward as the maxima lie at the ends of the range of integration, but the integrand is periodic so we can shift the range of integration without affecting its value, so we have

$$\begin{aligned}
F(\lambda, \theta, \theta') &= e^{a\lambda^2 \cos^2(\theta' - \theta)} \int_0^{2\pi} d\varphi' \exp \left[-4a\lambda^2 \sin \theta \sin \theta' \cos^2(\varphi'/2) \left(\sin \theta \sin \theta' \sin^2(\varphi'/2) + \cos \theta \cos \theta' \right) \right] H(\cos \theta' \cos \theta) \\
&\quad + e^{a\lambda^2 \cos^2(\theta' + \theta)} \int_{-\pi}^{\pi} d\varphi' \exp \left[-4a\lambda^2 \sin \theta \sin \theta' \sin^2(\varphi'/2) \left(\sin \theta \sin \theta' \cos^2(\varphi'/2) - \cos \theta \cos \theta' \right) \right] H(-\cos \theta' \cos \theta),
\end{aligned} \tag{J8}$$

and the maximum of the second integrand lies at $\varphi' = 0$.

b. Large λ limit for φ' integral

As λ is increased, we can approximate the exponent in the integral by its behaviour in the neighbourhood of $\varphi' = \pi$, and for the second integral, in the neighbourhood of $\varphi' = 0$. This is just using the method of steepest descent. Thus we get

$$\begin{aligned}
F(\lambda, \theta, \theta') &\sim e^{a\lambda^2 \cos^2(\theta' - \theta)} \int_0^{2\pi} d\varphi' \exp \left[-a\lambda^2 \sin \theta \sin \theta' \cos(\theta' - \theta)(\varphi' - \pi)^2 \right] H(\cos \theta' \cos \theta) \\
&\quad + e^{a\lambda^2 \cos^2(\theta' + \theta)} \int_{-\pi}^{\pi} d\varphi' \exp \left[a\lambda^2 \sin \theta \sin \theta' \cos(\theta' + \theta)\varphi'^2 \right] H(-\cos \theta' \cos \theta).
\end{aligned} \tag{J9}$$

Note that the exponents are still negative throughout the range of integration. This follows from the fact that $\sin \theta' \sin \theta \geq 0$ and for $\cos \theta' \cos \theta > 0$, we have $\cos(\theta' - \theta) = \sin \theta' \sin \theta + \cos \theta' \cos \theta > 0$, and similarly for the term with $\cos \theta' \cos \theta < 0$ we find $\cos(\theta' + \theta) < 0$.

For large λ this becomes

$$\begin{aligned}
F(\lambda, \theta, \theta') &\sim e^{a\lambda^2 \cos^2(\theta' - \theta)} R_-(\theta', \theta) H(\cos \theta' \cos \theta) \int_0^{2\pi} d\varphi' \delta(\varphi' - \pi) \\
&\quad + e^{a\lambda^2 \cos^2(\theta' + \theta)} R_+(\theta', \theta) H(-\cos \theta' \cos \theta) \int_{-\pi}^{\pi} d\varphi' \delta(\varphi').
\end{aligned} \tag{J10}$$

where

$$R_{\pm}(\theta', \theta) = \sqrt{\frac{\pi}{a\lambda^2 |\sin \theta' \sin \theta \cos(\theta' \pm \theta)|}}. \quad (\text{J11})$$

Writing $F(\lambda, \theta, \theta')$ in this way suggests that in the limit of large λ , the overwhelming contribution to the partition function comes from spin orientations for which $\varphi' = 0$ or $\varphi' = \pi$.

c. The θ' integral for large λ

We now have to deal with the integral

$$\begin{aligned} Z_S^{\text{cl}} &\sim Z_0^{\text{cl}} \int_0^\pi d\theta' \sin \theta' e^{\beta\omega_L S_0 \cos \theta'} \\ &\times \left[e^{a\lambda^2 \cos^2(\theta' - \theta)} R_{-}(\theta', \theta) H(\cos \theta' \cos \theta) \int_0^{2\pi} d\varphi' \delta(\varphi' - \pi) \right. \\ &\left. + e^{a\lambda^2 \cos^2(\theta' + \theta)} R_{+}(\theta', \theta) H(-\cos \theta' \cos \theta) \int_{-\pi}^{\pi} d\varphi' \delta(\varphi') \right]. \end{aligned} \quad (\text{J12})$$

where for later interpretation purposes, the φ' integrals will be retained unevaluated. This can be written

$$\begin{aligned} Z_S^{\text{cl}} &\sim Z_0^{\text{cl}} e^{a\lambda^2} \int_0^\pi d\theta' \sin \theta' e^{\beta\omega_L S_0 \cos \theta'} \\ &\times \left[e^{-a\lambda^2 \sin^2(\theta' - \theta)} R_{-}(\theta', \theta) H(\cos \theta' \cos \theta) \int_0^{2\pi} d\varphi' \delta(\varphi' - \pi) \right. \\ &\left. + e^{-a\lambda^2 \sin^2(\theta' + \theta)} R_{+}(\theta', \theta) H(-\cos \theta' \cos \theta) \int_{-\pi}^{\pi} d\varphi' \delta(\varphi') \right]. \end{aligned} \quad (\text{J13})$$

and once again the exponents in the integrand are all negative. The zeroes of the exponents will occur within the range of integration for $\theta' = \theta$ for the first exponents, and for $\theta' = \pi - \theta$ for the second. We can then approximate this by

$$\begin{aligned} Z_S^{\text{cl}} &\sim Z_0^{\text{cl}} e^{a\lambda^2} \int_0^\pi d\theta' \sin \theta' e^{\beta\omega_L S_0 \cos \theta'} \\ &\times \left[e^{-a\lambda^2 (\theta' - \theta)^2} R_{-}(\theta', \theta) H(\cos \theta' \cos \theta) \int_0^{2\pi} d\varphi' \delta(\varphi' - \pi) \right. \\ &\left. + e^{-a\lambda^2 (\theta' + \theta - \pi)^2} R_{+}(\theta', \theta) H(-\cos \theta' \cos \theta) \int_{-\pi}^{\pi} d\varphi' \delta(\varphi') \right], \end{aligned} \quad (\text{J14})$$

which becomes, in the large λ limit,

$$\begin{aligned} Z_S^{\text{cl}} &\rightarrow \tilde{Z}_{\text{S,US}}^{\text{cl}} \sim Z_0^{\text{cl}} e^{a\lambda^2} \sqrt{\frac{\pi}{a\lambda^2}} \int_0^\pi d\theta' \sin \theta' e^{\beta\omega_L S_0 \cos \theta'} \\ &\times \left[\delta(\theta' - \theta) R_{-}(\theta', \theta) H(\cos \theta' \cos \theta) \int_0^{2\pi} d\varphi' \delta(\varphi' - \pi) \right. \\ &\left. + \delta(\theta' + \theta - \pi) R_{+}(\theta', \theta) H(-\cos \theta' \cos \theta) \int_{-\pi}^{\pi} d\varphi' \delta(\varphi') \right] \\ &= Z_0^{\text{cl}} \frac{\pi e^{a\lambda^2}}{a\lambda^2} \int_0^\pi d\theta' e^{\beta\omega_L S_0 \cos \theta'} \left[\int_0^{2\pi} d\varphi' \delta(\theta' - \theta) \delta(\varphi' - \pi) + \int_{-\pi}^{\pi} d\varphi' \delta(\theta' + \theta - \pi) \delta(\varphi') \right]. \end{aligned} \quad (\text{J15})$$

which suggests that in the large λ limit, the spin orients itself in either the $\theta' = \theta, \varphi' = \pi$ or $\theta' = \pi - \theta, \varphi' = 0$ directions, though with different weightings for the two directions. Thus, for $0 < \theta < \pi/2$

If we return to the interaction on which this result is based, that is

$$V = (S_z \cos \theta - S_x \sin \theta) B = \mathbf{S} \cdot B(-\sin \theta \mathbf{x} + \cos \theta \mathbf{z}) = \mathbf{S} \cdot \mathbf{B}, \quad (\text{J16})$$

we see that the vector $-\sin \theta \mathbf{x} + \cos \theta \mathbf{z}$ has the polar angles $\theta' = \theta, \varphi' = \pi$. But as B can be fluctuate between positive or negative values, the vector \mathbf{B} can fluctuate between this and the opposite direction $\theta' = \pi - \theta, \varphi' = 0$. So the effect of the ultrastrong noise is to force the spin to orient itself in either of these two directions.

d. *Partition function in the large λ limit*

Returning to the expression for the partition function, we have

$$\tilde{Z}_{S,US}^{cl} \sim Z_0'' (e^{\beta\omega_L S_0 \cos \theta} + e^{-\beta\omega_L S_0 \cos \theta}) \propto \cosh(\beta\omega_L S_0 \cos \theta), \quad (J17)$$

where extraneous factors have been absorbed into Z_0'' . Further, to get at $\langle S_z \rangle$ we need

$$\langle S_z \rangle = S_0 \frac{\int_0^\pi d\theta' \cos \theta' F(\lambda, \theta', \theta)}{\int_0^\pi d\theta' F(\lambda, \theta', \theta)} = S_0 \cos \theta \tanh(\beta\omega_L S_0 \cos \theta). \quad (J18)$$

These results are of the same form as found for quantum spin half. That result is understandable given that the spin half would have two orientations, which mirrors the two orientations that emerge in the strong coupling limit here in the classical case.

2. Quantum ultrastrong coupling limit

The aim here is to derive an expression for the quantum MFG state of a spin S_0 particle coupled to a thermal reservoir at a temperature β^{-1} , (I20)

The ultrastrong coupling limit is achieved by making λ very much greater than all other energy parameters of the system, in effect, $\lambda \rightarrow \infty$. However, note the absence of the ‘counter-term’ $-\lambda^2(\cos \theta S_z - \sin \theta S_x)^2 Q$ in the above Hamiltonian. This term appears in [33], where it is found to be cancelled in the strong coupling limit when the trace over the reservoir states is made. Here, that cancellation will not take place, so its presence must be taken into account. It will have no impact in the case of $S_0 = \frac{1}{2}$, as this will be a c-number contribution, but it will have an impact otherwise.

With $H_S = -\omega_L S_z$ and $P_{s_\theta} = |s_\theta\rangle\langle s_\theta|$ the projector onto the eigenstate $|s_\theta\rangle$ of S_θ where

$$S_\theta = \cos \theta S_z - \sin \theta S_x; \quad S_\theta |s_\theta\rangle = s_\theta |s_\theta\rangle \quad (J19)$$

we have, in the ultrastrong coupling limit, the unnormalised MFG state of the particle

$$\tilde{\rho} = \exp \left[-\beta \sum_{s_\theta=-S_0}^{S_0} P_{s_\theta} H_S P_{s_\theta} \right] \exp[\beta \lambda^2 S_\theta^2 Q] = \sum_{s_\theta=-S_0}^{S_0} P_{s_\theta} \exp[-\beta \langle s_\theta | H_S | s_\theta \rangle] \exp[\beta \lambda^2 \gamma^2 s_\theta^2 Q]. \quad (J20)$$

Note, as a consequence of the absence of a counter-term, the contribution $\exp[\beta \lambda^2 S_\theta^2 Q]$ is not cancelled.

Further note the limits on the sum are $\pm S_0$. This follows since $S_\theta = \cos \theta S_z - \sin \theta S_x$ is just S_z rotated around the y axis, i.e.,

$$\cos \theta S_z - \sin \theta S_x = e^{i\theta S_y} S_z e^{-i\theta S_y} = S_\theta \quad (J21)$$

so the eigenvalue spectrum of S_θ will be the same as that of S_z , i.e., $s_z = -S_0, -S_0 + 1, \dots, S_0 - 1, S_0$. The eigenvectors of S_θ are then, from $S_z |s_z\rangle = s_z |s_z\rangle$

$$S_\theta e^{i\theta S_y} |s_z\rangle = s_z e^{i\theta S_y} |s_z\rangle \quad (J22)$$

i.e., the eigenvectors of S_θ are

$$|s_\theta\rangle = e^{i\theta S_y} |s_z\rangle; \quad s_\theta = s_z = -S_0, -S_0 + 1, \dots, S_0 - 1, S_0. \quad (J23)$$

We then have

$$\langle s_\theta | H_S | s_\theta \rangle = \omega_L \langle s_z | e^{-i\theta S_y} S_z e^{i\theta S_y} | s_z \rangle = \omega_L \langle s_z | \cos \theta S_z + \sin \theta S_x | s_z \rangle = \omega_L s_z \cos \theta \quad (J24)$$

from which follows

$$\tilde{\rho} = \sum_{s_z=-S_0}^{S_0} e^{i\theta S_y} |s_z\rangle \langle s_z| e^{-i\theta S_y} e^{\beta\omega_L s_z \cos \theta} e^{\beta\lambda^2 Q s_z^2}. \quad (J25)$$

The partition function is then given by

$$\tilde{Z}_S^{\text{qu}} = \sum_{s_z=-S_0}^{s_z=S_0} e^{\beta\omega_L s_z \cos \theta} e^{\beta\lambda^2 Q s_z^2}. \quad (J26)$$

This cannot be evaluated exactly, but the limit of large λ is yet to be taken. The dominant contribution to the sum in that limit will be for $s_z = \pm S_0$, so we can write

$$\tilde{Z}_{\text{S,US}}^{\text{qu}} e^{-\beta\lambda^2 Q S_0^2} \sim e^{\beta\omega_L S_0 \cos \theta} + e^{-\beta\omega_L S_0 \cos \theta} \propto \cosh(\beta\omega_L S_0 \cos \theta). \quad (\text{J27})$$

Apart from an unimportant proportionality factor, this is exactly the same results as found for the classical case in the limit of ultrastrong coupling, (J17).

In fact, if we follow the same procedure as above for the normalised density operator, we have

$$\rho = \frac{\sum_{s_z=-S_0}^{S_0} e^{i\theta S_y} |s_z\rangle \langle s_z| e^{-i\theta S_y} e^{\beta\omega_L s_z \cos \theta} e^{\beta\lambda^2 Q s_z^2}}{\sum_{s_z=-S_0}^{S_0} e^{\beta\omega_L s_z \cos \theta} e^{\beta\lambda^2 Q s_z^2}}. \quad (\text{J28})$$

The dominant contribution in the limit of large λ will then be for $s_z = \pm S_0$, so we get

$$\rho = \frac{e^{i\theta S_y} |S_0\rangle \langle S_0| e^{-i\theta S_y} e^{\beta\omega_L S_0 \cos \theta} + e^{i\theta S_y} |-S_0\rangle \langle -S_0| e^{-i\theta S_y} e^{-\beta\omega_L S_0 \cos \theta}}{e^{\beta\omega_L S_0 \cos \theta} + e^{-\beta\omega_L S_0 \cos \theta}}. \quad (\text{J29})$$

To work this out for arbitrary spin would require introducing the matrix elements of the rotation matrices for $\exp[-i\theta S_y]$, which would be a complex business. Instead we will simply introduce

$$\sigma_{\pm}(\theta) = e^{i\theta S_y} (|S_0\rangle \langle S_0| \pm |-S_0\rangle \langle -S_0|) e^{-i\theta S_y}, \quad (\text{J30})$$

and write this as

$$\rho = \frac{1}{2} [\sigma_+(\theta) + \sigma_-(\theta) \tanh(\beta\lambda\omega_L S_0 \cos \theta)]. \quad (\text{J31})$$

For $S_0 = \frac{1}{2}$ this above general result reduces to the earlier obtained result (for which the counter-term can be safely ignored), which is

$$\rho = \frac{1}{2} [1 + \sigma(\theta) \tanh(\frac{1}{2}\beta\omega_L \cos \theta)], \quad (\text{J32})$$

where $\sigma_+(\theta) = 1$ and $\sigma(\theta) = \cos \theta \sigma_z - \sin \theta \sigma_x$ and for which $\langle S_z \rangle = \frac{1}{2} \cos \theta \tanh(\frac{1}{2}\beta\lambda\omega_L \cos \theta)$ and $\langle S_x \rangle = \frac{1}{2} \sin \theta \tanh(\frac{1}{2}\beta\lambda\omega_L \cos \theta)$.